Pressure oscillations during start and stop of a high head Francis turbine

Anders Mathias Tørklep

MASTER THESIS

for

Anders Tørklep

Spring 2012

Pressure oscillations during start and stop of a high head Francis turbine

Trykkpulsasjoner i en høytrykks Francis turbin under start-stopp

Background and objective

In the last decade, the Norwegian hydropower turbines have experienced some cases of fatigue cracks in high head Francis turbine runners. The fatigue loads originate from the pressure oscillation caused by the blade passing of the runner- and guide vane, the draft tube swirl flow and from the start-stop operation of the turbine. During start/stop operation, the turbine goes the performance diagram where the pressure pulsations are severe compared with normal performance.

This work will measure and analyse the pressure oscillations in a model turbine that are installed in the Waterpower laboratory at NTNU during start/stop operation

The following tasks are to be considered:

1 Literature study

2 Suggest and make changes in the test rig in order to do dynamic measurements during start and stop

3 Instrumentation

4 Start-stop measurements of a turbine
- a. Carry out calibration of the pressure transducers that will be used in the pressure oscillation tests
- b. Carry out pressure oscillation measurements in the following areas during start-stop and normal operation:
    - i. Between the guide vanes and the runner
    - ii. Runner (if available)
    - iii. Draft tube

Within 14 days of receiving the written text on the master thesis, the candidate shall submit a research plan for his project to the department.

When the thesis is evaluated, emphasis is put on processing of the results, and that they are presented in tabular and/or graphic form in a clear manner, and that they are analyzed carefully.

The thesis should be formulated as a research report with summary both in English and Norwegian, conclusion, literature references, table of contents etc. During the preparation of the text, the candidate should make an effort to produce a well-structured and easily readable report. In order to ease the evaluation of the thesis, it is important that the cross-references are correct. In the making of the report, strong emphasis should be placed on both a thorough discussion of the results and an orderly presentation.
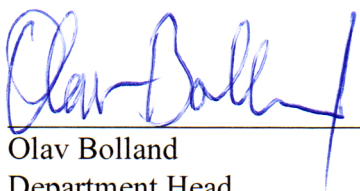
The candidate is requested to initiate and keep close contact with his/her academic supervisor(s) throughout the working period. The candidate must follow the rules and regulations of NTNU as well as passive directions given by the Department of Energy and Process Engineering.
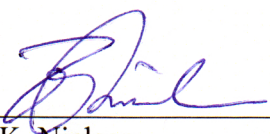
Risk assessment of the candidate's work shall be carried out according to the department's procedures. The risk assessment must be documented and included as part of the final report. Events related to the candidate's work adversely affecting the health, safety or security, must be documented and included as part of the final report.

Pursuant to "Regulations concerning the supplementary provisions to the technology study program/Master of Science" at NTNU §20, the Department reserves the permission to utilize all the results and data for teaching and research purposes as well as in future publications.

The final report is to be submitted digitally in DAIM. An executive summary of the thesis including title, student's name, supervisor's name, year, department name, and NTNU's logo and name, shall be submitted to the department as a separate pdf file. Based on an agreement with the supervisor, the final report and other material and documents may be given to the supervisor in digital format.

Department of Energy and Process Engineering, 10. January 2012

Olav Bolland
Department Head

Torbjørn K. Nielsen
Academic Supervisor

Preface

All work concerning this master thesis was carried out at the Waterpower Laboratory at Norwegian University of Science and Technology (NTNU). On account of all the people at the laboratory, this has been an extraordinary environment. Thank you all.

Part of the experimental planning and testing was conducted in collaboration with Luleå University of technology (LTU) and professor Michel Cervantes and PHD students Kaveh Amiri and Chirag Trivedi. Thank you for all the interesting conversations.

I would like thank Audun Tovslid for precious collaboration in the laboratory.

I would also like to thank Bård Brandåstrø, Joar Grilstad, Halvor Haukvik and Trygve Opland for all the assistance in the laboratory.

Thanks to Ole Gunnar Dalhaug for taking an interest in my work.

Huge thanks to my supervisor Torbjørn Nielsen for his invaluable expertise.

Finally I would like to thank my parents for being utterly awesome.

Anders Mathias Tørklep

Trondheim June 2012

Abstract

Start and stop procedures affect pressure oscillations throughout a hydropower plant. A desire to study how pressure oscillations behave during these dynamic conditions was the basis of this report. Instrumentation, experimentation and measurement analysis was conducted on a Francis model turbine in the Waterpower Laboratory at NTNU.

Eight pressure transducers were calibrated and used during the experiments. Two transducers were installed in the draft tube below the turbine. One was placed in the vaneless space between the guide vanes and the impeller vanes. Three pressure transducers on an impeller vane and two transducers located at the inlet were also included in the experiments.

Frequency analysis (PSD) was carried out for all the measurements to explore various pressure oscillations.

Except for the low frequent oscillations (< 30 Hz), definite frequencies repeatedly dominated the frequency domain during start/stop as well as for steady state operation.

The impeller vane oscillation showed an increase in pressure amplitude during guide vane closing. A bigger amplitude increase was registered for BEP than for part load and full load operation.

The guide vane frequency was located in and only in the runner. The amplitude of the guide vane frequency was significant and was located for all studied operational points. The power of this oscillation decreased during guide vane closing.

One specific frequency arose the question of an overtone phenomenon for the water hammer oscillation, a phenomenon, were the fundamental frequency is three times higher than the customary water hammer frequency.

Sammendrag

Start og stopp prosedyrer vil påvirke trykkpulsasjoner gjennom de ulike delene av et vannkraftverk. Et ønske om å kartlegge oppførselen til trykkpulsasjoner i løpet av disse dynamiske forholdene lå til grunn for denne oppgaven. Instrumentering, testing og analyse av data ble utført på en Francis modellturbin ved Vannkraftlaboratoriet på Norges Tekniske og Naturvitenskapelige Universitet (NTNU).

Totalt åtte trykktransdusere ble benyttet til innsamling av data. To transdusere ble installert i sugerøret og en transduser i omdreiningshulerommet mellom ledeskovler og løpehjul. I tilegg ble tre trykktransdusere på bladene på løpehjulet benyttet og to transdusere som var installert ved innløpet til turbinen.

Frekvensanalyse (PSD) ble anvendt for alle målingene for å finne ulike trykkpulsasjoner og deres amplituder.

Sett bort ifra lav frekvente pulsasjoner (< 30 Hz) var det enkelte frekvenser som gang på gang dominerte i frekvensplanet. Dette gjaldt både ved stasjonær og dynamisk kjøring.

Løpeskovlfrekvensen viste en betydelig økning i trykkamplituden under ledeskovlslukking. En større amplitudeøkning ble funnet for beste virkningsgard sammenliknet med del last og fullast.

Ledeskovlsfrekvensen ble detektert i løpehjulet. Trykkamplituden til denne pulsasjonen var betydelig og ble detektert for alle driftspunkt. Amplituden ble redusert når ledeskovlene ble lukket.

En spesiell frekvens reiste spørsmålet om et overtonefenomen for trykkstøt. Et fenomen hvor den fundamentale frekvensen er tre ganger størrelsen til den sedvanlige trykkstøtfrekvensen.

Table of contents

Contents

List of figures

Symbols

Symbol	Explanation	Unit
n	Rotational speed	Rpm
D	Diameter	m
Q	Volume flow	m^3/s
H	Nominal Head	m
P	Power	Watt
g	Gravitational acceleration	m/s^2
f	Impeller frequency	Hz $=1/s$
f_{iv}	Impeller vane frequency	Hz $=1/s$
f_{av}	Guide vane frequency	Hz $=1/s$
f_R	Rheingans frequency	Hz $=1/s$
z_{im}	Number of impeller vanes	-
z_{av}	Number of guide vanes	-
f_s	Sampling frequency	Hz $=1/s$
f_m	Signal frequency	Hz $=1/s$
f_{wh}	Water hammer frequency	Hz$=1/s$
f_{ut}	U-tube frequency	Hz$=1/s$
ω	Angular velocity	rad/s
a	Speed of sound	m/s
l	Length	m
Ned	Specific speed	-
Ned*	Specific speed at Best efficiency point	-
Qed	Specific discharge	-
Qed*	Specific discharge at Best efficiency point	-
α	Guide vane angle	degree
η	Efficiency	%
T	Time	s
ρ	Density	kg/ m^3
λ	Wavelength	m
v	speed	m/s
I	Moment of inertia	Kgm²

1. Introduction

The energy market has faced quite some changes in recent years. These changes have in various ways also influenced the operational patterns of hydropower plants. The need to adapt to changes in the market consequently leads to increased operation time outside of the best efficiency point. There is also a need for more frequent start up and shutdown procedures. This development will naturally increase the wearing down of various technical units. Any unit exposed to dynamic mechanical strain will be in risk of fatigue damage. The dynamic strains are pressure variations which cause the tension in the materials to vary. During every start/stop operation, turbines will experience pressure oscillations which differ from steady state operation. Some units will experience a severe increase in pressure oscillation power which in some cases may lead to fatigue cracks.

This report will explore the subject of pressure oscillation during start/stop operation for a model Francis turbine. The intent of this work is to first conduct instrumentation and experiments at the Waterpower laboratory at NTNU and perform data analyzes of the measurements.

2. **Previous work**

Pressure oscillation in hydropower is a subject which has been known and studied for a long time. W. J. Rheingans studied the pressure oscillations from the draft tube vortex as early as in the 1940s (Rheingans, 1940).

In more recent years there has also been done much work on the subject at the Waterpower Laboratory at NTNU. To mention a few; Kari Haugan (Haugan, 2007), Sindre Gidskehaug (Gidskehaug, 2010) and especially PhD Einar Kobro (Kobro, 2010) have all studied pressure oscillations in Francis turbines at NTNU. All these works were performed with respect to different operational points at steady state. Pressure oscillations during start/stop operations for a Francis turbine is a less explored subject. No previous work was to be found for a direct comparison.

3. Theory

3.2 Pressure oscillations in Francis turbines

Fatigue damage caused by pressure variations during start and stop is a considerable matter for certain parts in the system. For Francis turbines especially the master valve and the spiral casing are proven to have an increased likelihood of cracking (Bakken, et al., 2001). Pressure variations for these two components are recognized by low frequency of pressure oscillations. The runner on the other hand is recognized by higher frequency of pressure oscillations.

Pressure oscillations are a natural phenomenon in hydraulic machinery. A pressure oscillation implies an unstable pressure and flow field and can occur periodically or stochastically. This occurs when the flow field is affected by the waterway throughout the machine. The magnitude of the oscillations is determined by design, operational pattern and dynamic response. The vibrations caused by oscillations will cause fatigue damages over time. Powerful pressure oscillations are a very common operational problem for Francis turbines.

Pressure oscillations can originate directly from turbine rotation (rotational fluctuations) or from system inequality (elastic fluctuations).

3.2.1 Rotational fluctuations

Pressure oscillation may occur in many different parts of a system and the sources of oscillations can be many. The most common low-frequency pressure oscillation for a hydropower system is caused by the draft tube vortex (IEC, 1999). In 1940 W. J. Rheingans found that oscillations in vacuum or pressure in the draft tube (Rheingans frequency) caused oscillations in the effective head which again caused oscillations in the power efficiency (Rheingans, 1940). From rotational effects it is typically four pressure oscillations which cause significantly high amplitudes (Haugen, 1994):

Impeller frequency

Equation 3-1

$$f = \frac{n}{60} \ [Hz]$$

The impeller frequency can give powerful impulses if the impeller vanes are damaged, the runner is unbalanced or if the flow is unsymmetrical.

Impeller vane frequency

$$f_{iv} = f \times z_{iv} \; [Hz]$$

This frequency is an oscillation which occurs every time an impeller vane passes the same guide vane. The amplitude from this oscillation is the dominating amplitude under stable operational conditions. The amplitude will also be influenced by the distance between the impeller and the guide vanes and therefore by guide vane opening.

Guide vane frequency

$$f_{gv} = f \times z_{gv} \; [Hz]$$

The guide vane frequency is caused by an impulse given by damage on the impeller. The impulse will occur every time the damaged part passes a guide vane.

Rheingans frequency

$$f_R \cong \frac{f}{3,6} \; [Hz]$$

The cause of Rheingans, or draft tube vortex frequency, is a mass fluctuation which occurs in the draft tube. Image 3.2-1 shows a visible Rheingans oscillation in the draft tube. The amplitude of the Rheingans frequency gets predominant only when the vortex is visible to the naked eye. This means when the pressure becomes so low that the vortex is filled with air.

Figure 3.2-1 – Draft tube or Rheingans vortex at the Waterpower laboratory

These four frequencies are according to Haugen the most predominant pressure oscillations in a hydropower system.

3.2.2   Elastic fluctuations

In addition to rotational effects, pressure oscillations can occur from system inequalities. These oscillations will be independent of the rotational speed of the impeller. Among these, the water hammer oscillation is one of the most common. Water hammer is a consequence of elastic fluctuations in the waterway system. Pressure changes in the waterway will cause the mechanical fluctuations to propagate in the water with the speed of sound. By any change in the pressure an impulse is initiated. As for instance, when the guide vanes angels in a hydropower plant are adjusted, the pressure will change and this will again initiate an oscillation. A water hammer oscillation can occur both upstream and downstream to the turbine.

According to Torbjørn Nielsen (Nielsen, 1990) the period of this pressure wave will be four times the length to the nearest water surface, divided by the speed of sound in water.

Equation 3-5

$$T_{wh} = \frac{4L}{a}$$

$$L = length\ to\ closest\ water\ surface, \quad a = speed\ of\ sound$$

This will result in the following frequency:

Equation 3-6

$$f_{wh} = \frac{a}{4l}$$

The background for this equation is explained in appendix E.

An important issue when studying the water hammer oscillation is the variation in the speed of sound (a). Sound will travel with different speed in different medium and it is dependent on density (ρ) and a coefficient of stiffness (K).

Equation 3-7

$$a = \sqrt{\frac{K}{\rho}}$$

Because of this the speed of sound may vary significantly for the same medium. The speed of sound in still water is found to be approximately 1450 m/s. In run-up tunnels to power plants it is found that a=1200 m/s is a good estimate (Nielsen, 1990). Even this may vary a lot due to variations in amount of confined air and rock quality. In extreme cases where huge amount of air is confined in a system the speed of sound can be as low as or lower than the speed of sound in air (approximately 340 m /s). The sound of speed in the laboratory at NTNU is not defined and will depend on which waterway system utilized. Therefore this may be a significant uncertainty when defining the water hammer frequency.

Another system oscillation is the u tube fluctuation. This mass oscillation may occur between free water surfaces. Odd Guttormsen (Guttormsen, 2006) defines the period for an ideal u-tube fluctuation as follows:

$$T = 2\pi \sqrt{\frac{l}{2g}}$$

l = length of water column [m]

The frequency of the ideal u-tube oscillation is expressed in equation 3-9.

$$f_{ut} = \frac{1}{T} = \frac{1}{2\pi \sqrt{\frac{l}{2g}}}$$

3.3 Frequency analysis

Most of the theory from this section is from the book "Introduction to Engineering Experimentation" by Anthony J. Weeler and Ahmad R. Ganji (Wheeler, et al., 2010). The mathematical description of the Fourier series and transform is well described in this book (to mention one source) and will not be included here.

Frequency is the rate of occurrence of a repeating event over time.

Equation 3-10

$$f = \frac{v}{\lambda}$$

f=frequency [Hz]   v = speed [m/s]   λ=wave length[m]

3.3.1   Discrete sampling and analysis

Digital sampling of a signal is always discontinuous or discrete. The consequence is that all the information between every sample is lost. The sampling frequency is what determines how frequent a sampling from the original signal occurs. An erroneous choice of the sampling frequency may consequently lead to faulty results. A tool to reconstruct the original signal is the sampling-rate theorem. This describes that the sampling rate needs to be at least the double of the highest frequency from the original signal.

3.3.2   Spectral analysis of time varying signals

Time varying signals often has complicated wave structures, but may be expressed as a set of sine and cosine waves at various frequencies. The method is called spectral analysis. The most utilized method within spectral analysis is the Fourier series analysis. Figure 3.3-1 shows how two waves (red) at different frequencies are added (blue) to adapt to an original triangle signal (black).
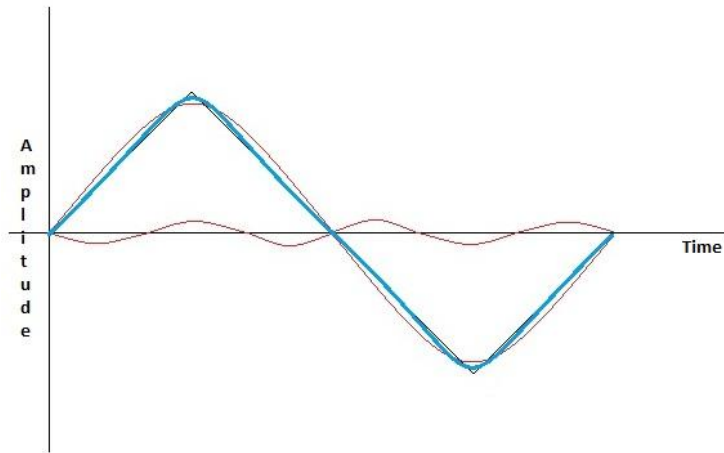
Figure 3.3-1 – Sine fitting of a triangle signal.

A Fourier series is that any periodic function can be expressed by a constant and a series of sine and cosine waves. Another method to find the spectral information in a signal is Fourier Transform. This is the method utilized in this report. The Fourier transform is a generalization of the Fourier series and can be used for all practical functions. The Fourier transform divides a function into its various frequency parts. It takes the original signal from the time domain to the frequency domain. In figure 3.3-2 the two domains are shown.

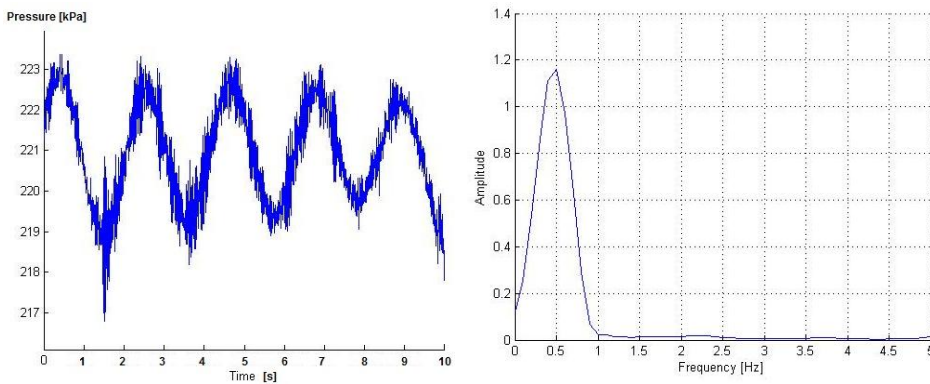**Figure 3.3-2 – Time domain (left) and frequency domain (right)**

The time domain to the left shows a pressure variation over 10 seconds. This is the actual measured signal. The figure on the right shows the enlarged frequency domain for low frequencies (0-5 Hz). A peak at approximately 0.5 Hz is the dominant frequency, which corresponds well with the approximately 5 dominant waves over 10 seconds in the time domain.

9

3.3.3 Window functions

The sampled value of a determined frequency component in the start of a sampling period will be different than the one on the end. This may lead to so called spectral leakage were the results shows significant coefficients for frequencies which may not be actual frequencies in the original signal. A window function reduces this effect. A window function dampens the signal in the start and end of the sampling period which is illustrated in figure 3.3-3 (Hanning window).
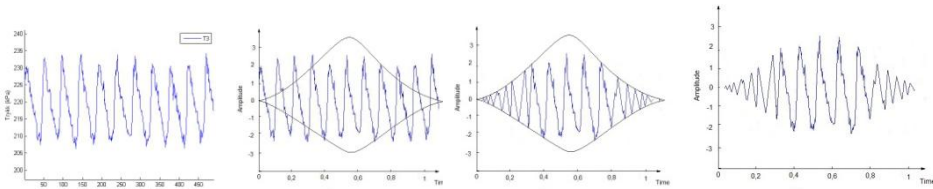
Figure 3.3-3 – Hanning Window function fitted to a signal

The negative effect of the window function is that it will also dampen the average amplitude from the original signal. The compromise between frequency resolution and amplitude will exist for all window functions.

3.3.4 Harmonies

It is very important to be aware of harmonies in frequency analysis. A harmony is normally an integer to the fundamental frequency. An example of sub harmonics in the frequency domain is seen in figure 3.3-4.

Figure 3.3-4 – Harmonies in the frequency domain

3.4 **Prototype versus model**

The major regulation issue of a hydroelectric power plant is the inertia of the mass of water. If the volume flow is decreased by closing the guide vanes the pressure H will severely increase because of the retardati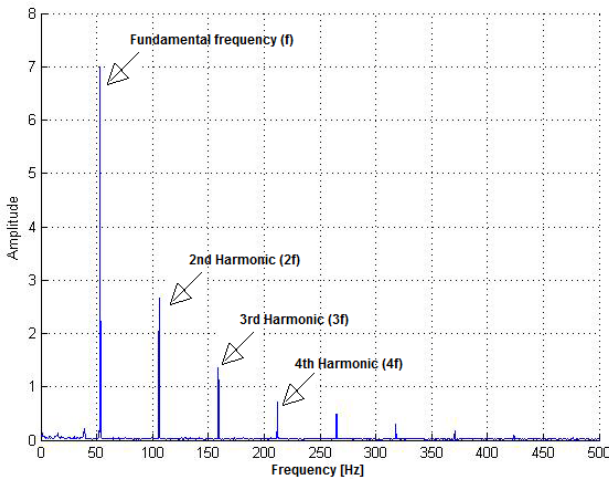on forces. This will immediately increase the power which is highly undesirable. Because of this, it is important that the inertia of the mass of water is held small. The inertia is related to the acceleration with a time constant. This time constant (T_W) express the inertia of the water mass. T_W is defined as the time it takes for the mass of water to accelerate from the closest water surface upstream of the turbine to the closest water surface downstream of the turbine.

Equation 3-11

$$T_w = \frac{Q}{gH} \sum \frac{l}{A}$$

The value of T_W should not be much higher than 1.0 to obtain a good regulation system (Nielsen, 1990).

Another important time constant concerning regulation is the oscillating mass constant T_A. This is the acceleration time for the impeller and the generator. These masses delay the increase in rotational speed. T_A is the time it takes for the generator and the impeller to obtain angular velocity ω_0 from a stand still.

Equation 3-12

$$T_a = J \times \frac{\omega_0^2}{P_{max}}$$

A common way to compare between different installations is through the use of dimensionless quantities. There are in fact several dimensionless quantities in use in the hydropower community. N_{ED} and Q_{ED} are two well established quantities. The N_{ED} is a dimensionless quantity for rotational speed, while the Q_{ED} is for discharge. Both are defined in the following equations.

Equation 3-13

$$N_{ED} = \frac{n \times D}{\sqrt{g \times H}}$$

$$Q_{ED} = \frac{Q}{D^2 \times \sqrt{g \times H}}$$

4. **Preparation and execution of measurements**

4.2 **Setup**

4.2.1 **Waterway**

All the tests were conducted at the Water power laboratory at NTNU. There are multiple ways to organize the pipelines to obtain various operating conditions. By the start of 2012 the laboratory setup for Francis and Reversible pump turbines was installed as a closed loop system where the water head could be adjusted by two 315 kW pumps. Because of the intended dynamic measurements an open loop system was needed to avoid the rotational influence from the pump. A section of this open loop system is seen in figure 4.1.
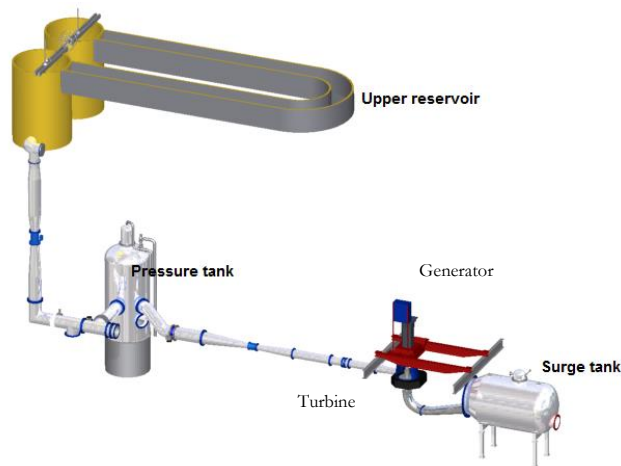
Figure 4.2-1 - A section of the open loop system at NTNU

Water from the lower reservoir is pumped up to the attic in the laboratory to create an upper reservoir with a free water surface. From there the water passes through a pressure tank and onwards to the turbine. To create a free water surface downstream from the turbine the surge tank had to be modified. An approximately 180 cm high steel plate was installed inside the surge tank to create a water surface just higher than the turbine (4 mm higher) as shown in figure 4.2.

Figure 4.2-2 - A drawing of the Francis rig setup with the installed steel plate in red
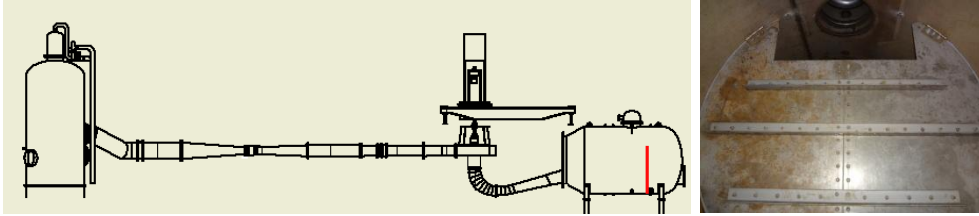
In addition a new pipe bend was created at the far end of the surge tank to guide the water straight down to the lower reservoir.

4.2.2   **Francis model turbine**

The turbine is installed on a vertical shaft with a 352 kW generator. For the open loop system there are two parameters (with constant head) to control the turbine. These two parameters are the rotational speed of the generator and the guide vane angle (α).

There are 28 guide vanes on the model turbine and Table 4-1 shows the closing time of these guide vanes in the Waterpower laboratory.

Guide vane angle – α	Time
14 to 0	7 s
10 to 0	5 s
7 to 0	3.5

Table 4-1 – Guide vane opening times

The Francis turbine installed at the Waterpower laboratory is a model turbine of Tokke power station. The model turbine has 30 impeller vanes in total, were 15 of these are splitters (Dahlhaug, 2007).

Even though pressure oscillations have been proven difficult to scale it was desirable to have a scalable setup. The closing time of the guide vanes divided with the time constant T_W (the inertia of the mass of the water) was utilized as a scaling parameter. After talks with employees at Tokke power station (Moen, 2012) the necessary data was obtained.

	Tokke power	Waterpower laboratory
Head [m]	377	12.3
Rotational speed [rpm]	375	332
Discharge [m^3/s] (full load)	31	0.27
Number of guide vanes (z_{GV})		28
Number of impeller vanes (z_{IV})		30
Tw	-Classified-	0.247 s*
Ta	-Classified-	0.85 s*
Tclose	-Classified-	7.5 s*
Tclose/Tw	30.7	30.4

*Calculations of the constant is found in appendix B

Table 4-2 – Data from Tokke power station and Waterpower laboratory

4.2.3 **Transducers and measurement equipment**

In total, eight pressure transducers were used during the experiments. Different systems for signal acquisition were needed because of the difference in pressure transducers and the variation of locations. Location and setup of all transducers will be presented.

Two pressure transducers were already calibrated and installed in the rig by Eve Walseth for an unrelated experiment. The placement of these two transducers can be seen in figure 4.2-3.
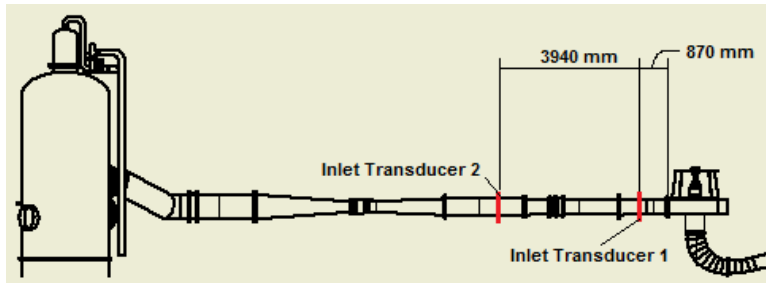

Figure 4.2-3 - Placement of inlet transducers

These two pressure transducers emit ±10 VDC (Volt Direct Current) signals which mean there was no need for an amplifier. Inlet transducer 1 and 2 was connected directly to the data acquisition system.

Figure 4.2-4 shows the location of two pressure transducers in the draft tube and one in the vaneless space between the guide vanes and runner vanes.
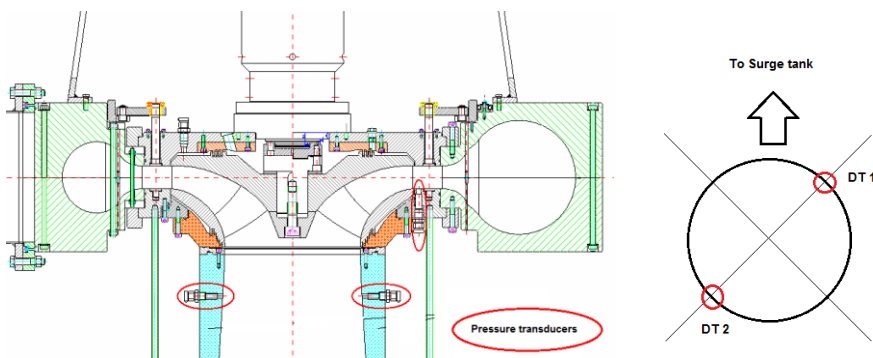

Figure 4.2-4 – Placement of draft tube transducers and vaneless space transducer

These three transducers have an electrical output of ±5 mVDC which needs signal amplification. An HBM amplifier changed the signal to ±10 Volt.

The final three pressure transducers used in the experiment was imbedded on the impeller vanes in the runner. Pressure transducers were by Einar Kobro installed along each side of the blade through one channel. 12 transducers on the pressure side and 12 transducers on the suction side were originally installed. Over time connection with 21 of these transducers has been lost and only 3 was operational for the experiment in this thesis. Figure 4.2-5 shows the placement of these 3 transducers and an image of two random transducers.
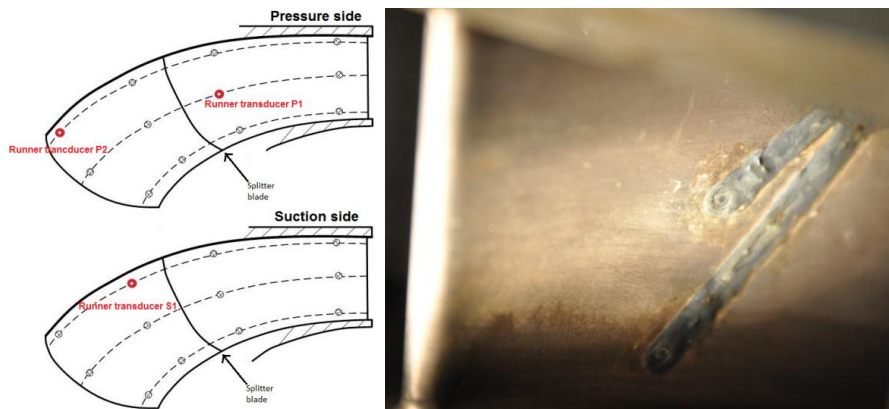
Figure 4.2-5 – Placement of runner transducers (left) Image of two transducers (right)

To log data from these runner transducers a cordless logging system was needed. The first system that was considered was a NI cRIO-9012 Real-time controller which exists at the Waterpower laboratory. This is a programmable unit which has been used for experiments at Tokke power plant. This system is relatively large in size and has never been tried out on the test rig at NTNU, which has considerably less installation space. For this reason a wireless system, also existing at the laboratory at NTNU, was chosen.
SRI/PMD series 500e is a digital telemetry system consisting of an eight channel transmitter and receiver. The receiver amplifies the signal and has both analog and digital output. The pressure transducers in the runner were connected to the telemetry transmitter which needs to be attached to the shaft of the turbine. The signal was transmitted to the telemetry receiver which again sent an analog signal to the NI acquisition system. This is the same system used by Einar Kobro in his doctoral thesis (Kobro, 2010).

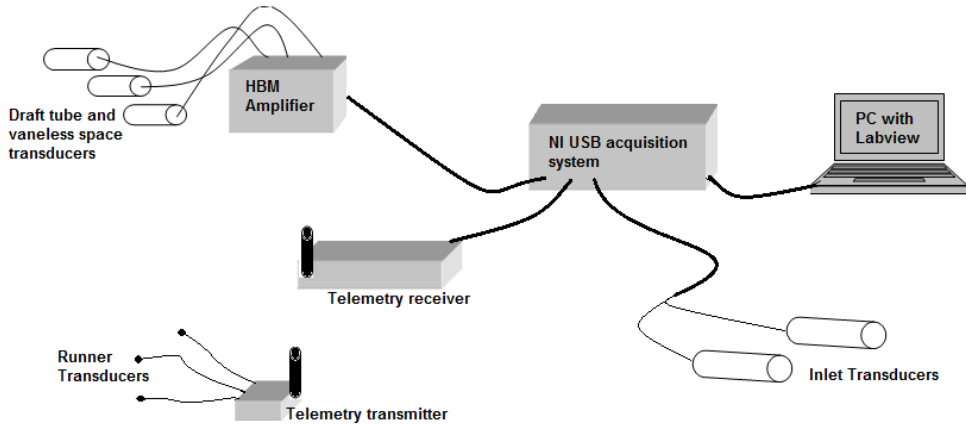The logging system for all the transducers can be seen in figure 4.2-6.

Figure 4.2-6 – Setup of all measurement equipment

A list of components used for data logging is displayed in table 4-3 and a list of transducers utilized in table 4-4.

Hardware	Type	Range	Bandwidth
PC with Labview	National Instruments Labview v11.0	Programmable	50k sampling per second
USB acquisition system	National Instruments NI-cDaq 9172		400k sampling per second
Analog input module to USB acquisition system	National Instruments 4-Channel, 24-Bit Ni 9239	± 10 V	50k sampling per second per channel
Amplifier	HBM - DCV measuring amplifier	± 10 V	10 kHz
Wireless transmitter	SRI-500e	± 2,5 V	17k sampling per second
Wireless receiver	SRI-500e	± 10 V	Compatible with transmitter

Table 4-3 – Hardware specifications

18

Transducer	Range[bar a]	Natural frequency	Number of transducers	Placement
Kulite XTE 190-T1	0 - 3.5	300 kHz	1	Draft tube cone
Kulite XTE 190-T1	0 – 7	380 kHz	1	Draft tube cone
Kulite XTE 190-T1	0 – 7	380 kHz	1	Vaneless space
Kulite LL080	0 – 3.5	300 kHz	3	Runner blade
Druck PTX 610	0-2.5	-	2	Upstream inlet

Table 4-4 – List of pressure transducers

4.3 **Calibration**

All the calibrations have been performed static and carried out at the Waterpower laboratory. Different calibration systems had to be used for the various pressure transducers. Deadweight testers were used for most pressure transducers except for the runner transducers. The runner transducers had to be calibrated while installed in the runner and a pressure tank was build and used for calibration. The whole process is explained in detail in appendix C An already existing Labview program at the Waterpower laboratory, copyright Håkon Hjort Francke, was used for logging calibration data. Reports including uncertainty, gain and offset equation from all executed calibrations are located in appendix D.

The use of the exact same hardware during calibration and actual measurements is a preference. For the acquisition hardware an USB log box (NI-USB 6211) was used during the calibration of runner, draft tube and vaneless space transducers. For the experimental measurements the signals went through a different USB acquisition system. The reason for the change was to gather as many signals into the same logging system and the setup in figure 4.2-6 was found to be the most practical.

4.4 **Pressure measurements**

Two parallel logging systems were used for all the tests carried out. One system is a permanent operating system for the Francis rig at the Waterpower laboratory. This measures several parameters with a relative low sampling frequency (approximately 1.5 Hz). This system was set to log data parallel to the customized logging system for all the pressure transducers.

All the data from the pressure transducers were logged on a customized Labview program (appendix F). The program used is a modified version of one of Einar Kobros programs. The program needed to be modified because of the amount of entry signals. Next to eight pressure signals, revolutions per minute, discharge, and differential pressure were included in the same logging program to have a better control during start and stop measurements. The Labview program uses calibrated gain and offset coefficients for all transducers to log the actual pressure.

Pressures from all transducers were logged at the same time with a constant logging frequency. When using discrete sampling, which was the case here, there is always a risk of logging "false" signals (Wheeler, et al., 2010). The sampling-rate theorem describes that the sampling frequency has to be twice the size as the highest expected frequency in the signal. For transient signals the sampling time should be 3-5 times the highest expected frequency (National Instruments, jun, 2011). The highest expected frequency is the impeller vane frequency which is 30 times the impeller frequency. The rotational speed of 332 rpm (Speed for measurements) would give an impeller vane frequency of 166 Hz. This results in a highest expected frequency of 166 Hz. The lowest sampling rate for the hardware was on the telemetry system. The sensor sample rate limit for the telemetry system is 2115 Hz for 4 channels at 16 bit (analog to digital resolution). A sampling frequency of 2005 Hz was chosen. This is a frequency that will be bigger than five times the highest expected frequency for all the intended measurements. In appendix F the whole Labview program can be studied.

The logging period varied from 20 seconds and up to 60 seconds, depending on the test. All data from all tests were logged and saved locally on the logging computer. All tests were run in collaboration with Chirag Trevedi and Audun Tovslid. The various tests performed will be explained in detail in section 4.5

4.5 **Testing**

All tests were conducted at the Waterpower laboratory at NTNU.

4.5.1 **Hill chart**

Ten different guide vane openings from 4 degrees to 14 degrees were chosen to construct a hill chart. For each guide vane opening, 15 different rotational speeds (0.15-0.22 Ned) were chosen. Each point was logged for 20 seconds. The results from the test were loaded into a Matlab script which was kindly given from PhD candidate Grunde Olimstad. The result can be seen in figure 5.1.

4.5.2 **Start and stop test**

Three points in the hill diagram were chosen, Part load, best operational point and full load (see figure 5.1). Before start and stop test a steady state measurement was carried out for each operational point. The steady state measurement was done after two minutes of steady operation and then a 20 seconds logging series   was performed. The start stop test was conducted in one logging series by running at steady state followed by closing procedures, starting procedures and back to steady state. The start stop measurement was conducted over a 60 seconds time period. A list of all the measurement steps follows and figure 4.5-1 shows the steps in a pressure/time diagram for one pressure transducer.

- Adjust to the given operational point.
- Start logging (60 second period)
- Step 1 - Steady state for approximately 5 seconds
- Step 2 - Closing guide vanes to a 0 degree angle
- Step 3 - Stabilization (5 seconds)
- Step 4 – Generator shutdown
- Step 5 - Stabilization (5 seconds)
- Step 6 – Generator start up
- Step 7 - Stabilization (5 seconds)
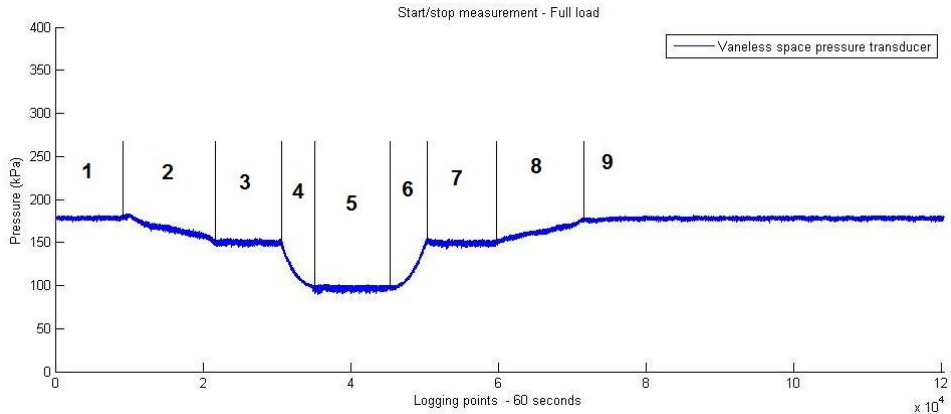- Step 8 – Opening guide vanes to initial state
- Step 9 – Stabilization

Figure 4.5-1 – Periods for the stop start measurements in a time domain for

4.5.3   Control testing

To be able to verify or refute certain frequencies two types of control tests were conducted.

One test was conducted with various occupancy levels of water in the pressure tank. The three different levels are shown in Figure 4.5-2. These tests were to verify or refute frequencies linked to elastic fluctuations in the system.
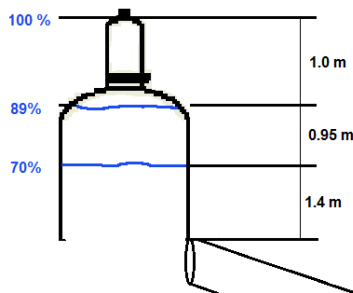

Figure 4.5-2 – Occupancy level of water in the pressure tank at the Waterpower laboratory

Another type of control was to run experiments for different rotational speeds. This was done to verify or refute frequencies related to rotational dependent frequencies like the impeller vane or guide vane frequency.

4.6 Data analyzing method

Matlab was used to analyze all the sampled data from the tests (appendix F). Instead of using Fast Fourier Transform (FFT), the somewhat more advance Matlab function Power Spectral Density (PSD) was utilized. Kobro found in his work (Kobro, 2006) that PSD didn't suffer from the same amount of low frequency noise as FFT did. The PSD function describes the same as the FFT but is an advantageous function when a high amount of noise is expected (Goldman, 1999).

An important difference in frequency analysis of steady state measurements and start stop measurements is its fundamental signal differences. Steady state signals have a deterministic and periodic waveform, while a signal from start or stop has a transient non-periodic wave form. For this reason it was decided to analyze the start and stop measurement series one period at a time. This breakdown is the same as for the start and stop procedures and is seen in figure 4.5-1. A disadvantage for the stop/start analysis is the relative small sample to the Fourier transform. The Frequency analysis for the steady state measurements is based on 40,000 logging points while the start stop had 4,000 points. 4,000 points (2 seconds) was chosen for each period in the start stop analysis. This was the highest number that would fit the smallest period. The period samples were chosen in such a manner that the all logging points fell within the transitions of periods (figure 4.6-1).
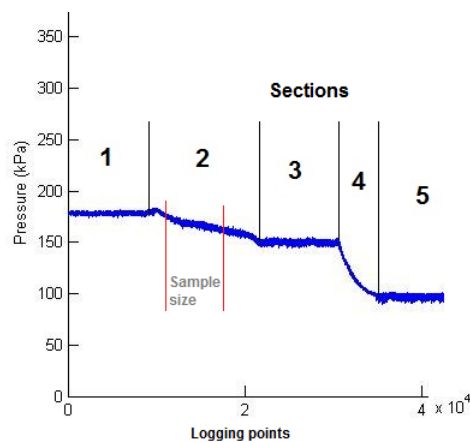

Figure 4.6-1 – Sampling for frequency analysis

Hanning was chosen as the operating window function in the analysis. Hanning is a window function suitable for various types of signals including some transient signals. National Instruments states that Hanning is a suitable function for "Transients whose duration is longer than the length of the window" (National Instruments, dec, 2011).

The amplitudes in the frequency domain were found to vary with the chosen window function and its window size. The amplitudes will indicate the power of the respective frequency, but no direct relationship was found (Tørklep, 2011). For this reason the amplitudes in the results should be evaluated against each other.

5. Experimental results and discussion

This section will present and discuss results from laboratory test executed at NTNU. Initially the developed hilldiagram will be presented. In section 5.3 the results from steady state measurements are found followed by start and stop measurement results.

5.2 Hill chart

In Figure5.2-1 the Hill chart of Tokke Francis model is shown. The hill chart is constructed of measurements executed on the 15th of May 2012 at the NTNU laboratory. Best efficiency point (BEP), part load and full load are marked in the figure while Table 5-1 displays the details for each operational point.
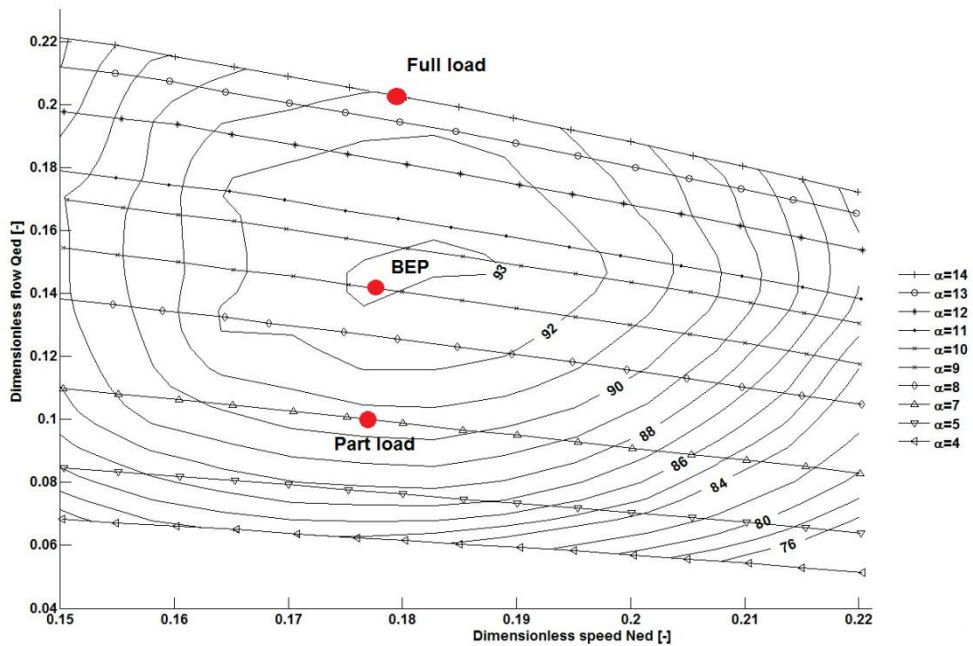
Figure5.2-1 Hill chart of Tokke model turbine in open loop system at Waterpower laboratory at NTNU. Constant Head=12,3m

	Q_{ED}	N_{ED}	N [rpm]	η [%]	α [degrees]
Part load	0.111	0.177	332	91.8	7.03
BEP	0.152	0.178	332	93.4	9.8
Full load	0.204	0.180	332	91.1	13.9

Table 5-1 Details of three operational points (part load, BEP and full load).

5.3 **Steady state**

This section will present results from steady state measurements. Due to similar results for all operational points, BEP will be the concentrated subject for discussion. Visual presentations of part load and full load can be seen in appendix A.

Eight pressure transducers were used during measurements. Figure 5.2 shows the root mean square (RMS) value of the absolute pressure for each pressure transducer and for the three operational points. The RMS is calculated from 20 seconds steady state measurements. The transducers in Figure 5.3-1 are placed in actual water column sequence.
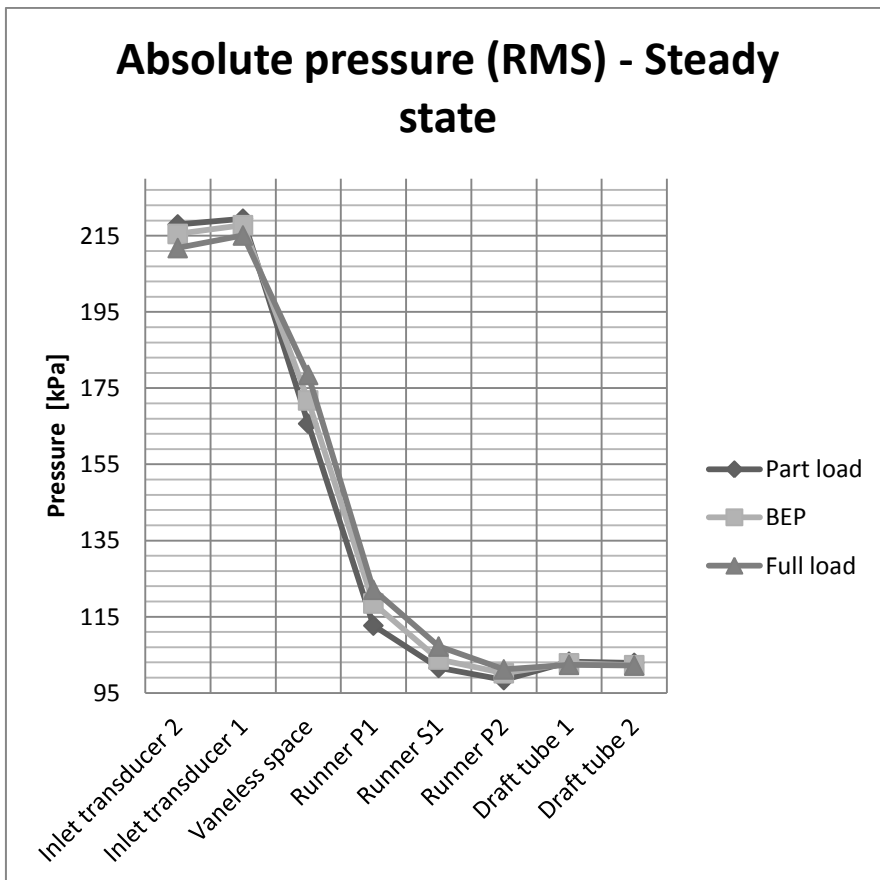
Figure 5.3-1 - Absolute pressure (RMS) along the water column at steady state

To take a closer look at the signals from the steady state measurements, Figure 5.3-2 displays signals from all eight pressure transducers. The y-axis displays absolute pressure while the x-axis displays 40,100 log points which denote 20 seconds (Sampling rate = 2005 Hz). Each of these four areas will be presented in the following sections. The four areas are as follows: the two transducers in front of the turbine, the vaneless space between guide vanes and the impeller, the tree transducers on the blade and the two transducers in the draft tube.
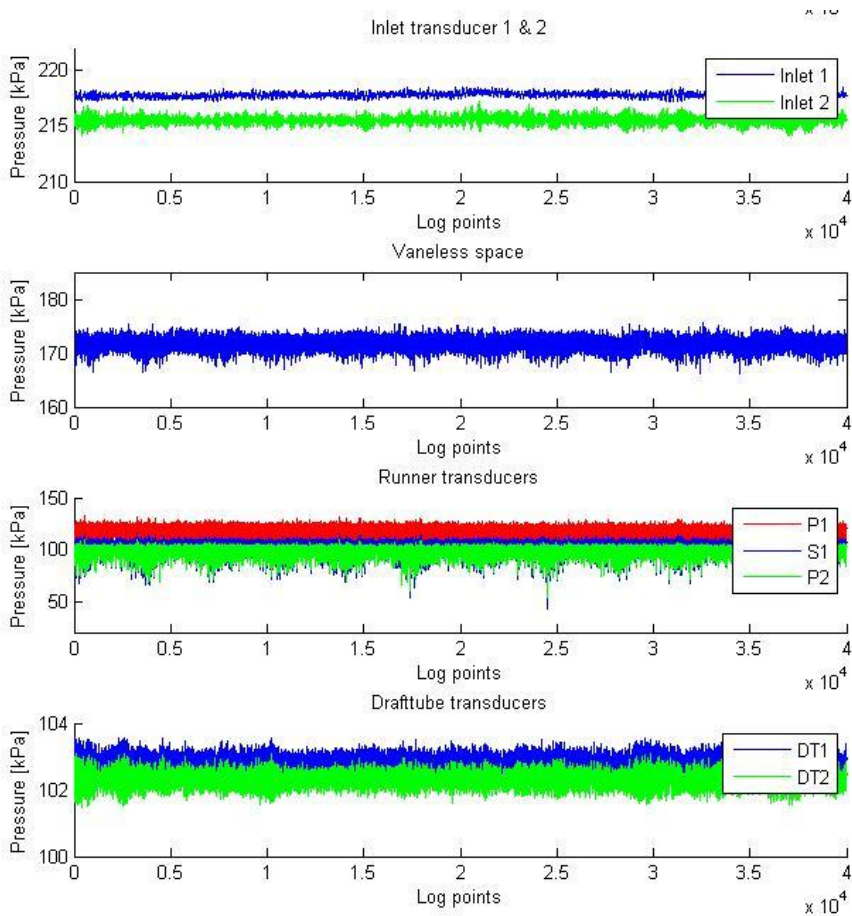
Figure 5.3-2 -Steady state –BEP – Time domain or 20 seconds
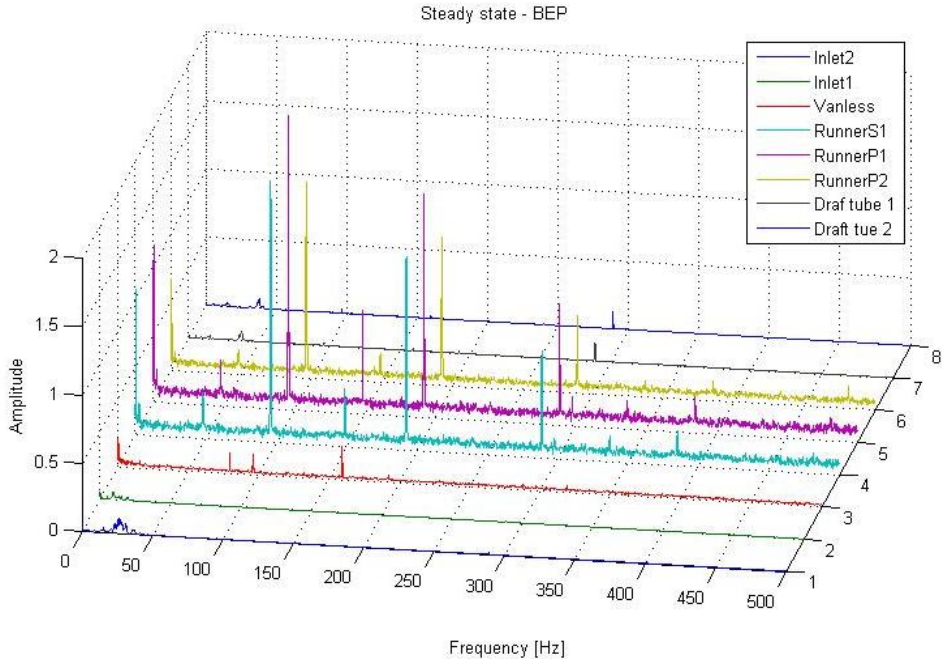
Figure 5.3-3 – Steady state – BEP – Frequency domain for all transducers

Figure 5.3-3 and Figure 5.3-2 clearly shows the significant different in amplitude power for the different transducers. Especially the three transducers in the runner excel with several frequencies with relatively high amplitudes.

Expected rotational dependent frequencies for BEP are seen in Table 5-2.

Rheingans frequency	1.3 – 1.8 Hz
Impeller frequency	5.53 Hz
Guide vane frequency	154.9 Hz
Impeller vane frequency	166 Hz

Table 5-2 – Theoretical frequencies at BEP and 332 rpm

28

5.3.1   **Inlet transducers**
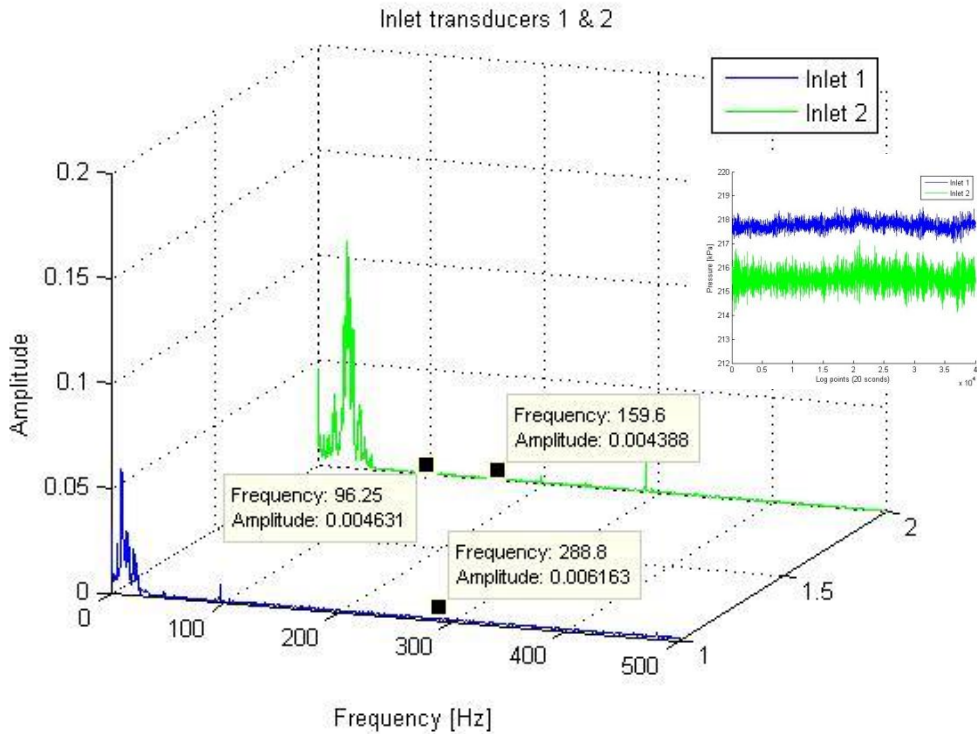
Figure 5.3-4 – Steady state – BEP – Frequency domain inlet transducers 1 & 2.

The two inlet transducers are mounted approximately 4 meters apart were Inlet transducers 1 is closest to the turbine. As seen in Figure 5.3-4 the dominating amplitudes on each transducer is relative low frequent. The amplitude peak for inlet transducer 1 is always located lower than for the inlet transducers 2. For this particular operational point the amplitude peaks in inlet transducers 1 and 2 are located at 10 Hz and 26 Hz respectively. These frequencies were found to be dependent on rotational speed and occupancy level in the pressure tank. No theoretical oscillations were found to match these frequencies.

Traces of three particular frequencies are seen in Figure 5.3-4. These frequencies (96.25, 159.6 and 288 Hz) will be discussed in detail later.

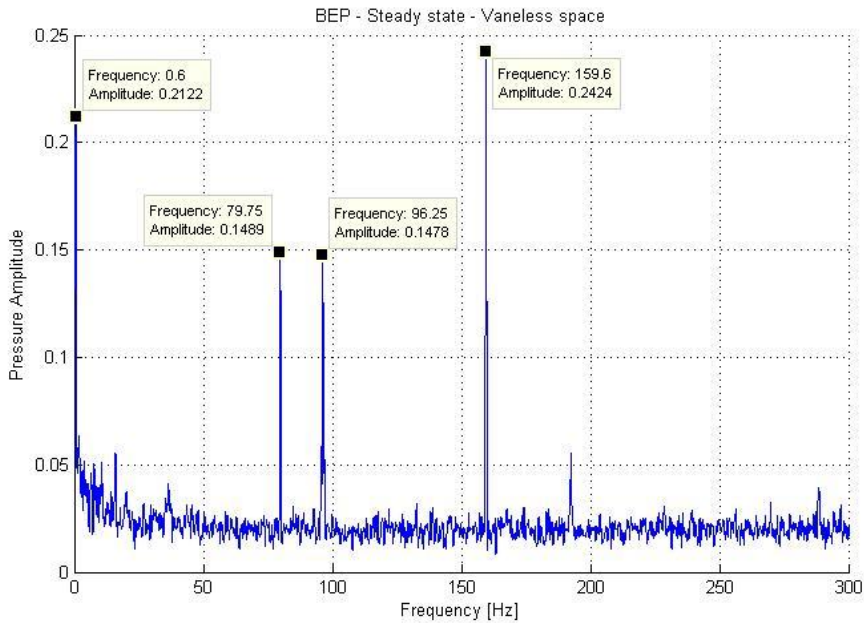### 5.3.2   **Vaneless space transducer**

Figure 5.3-5 – Steady state – BEP – Frequency domain vaneless space transducer.

From experience (Dahlhaug, 2007)(Tørklep, 2011) the impeller frequency is the most dominant frequency in the vaneless space. As seen in Figure 5.3-5 the most dominant frequency is 159.6 Hz with its likely half harmony (79.8 Hz). With a rotational speed of 332 rpm and 30 impeller vanes, the expected impeller frequency was 166 Hz. This deviation was found for various operational points and was always 4%. One possible explanation to this deviation is that there's a calibration error in the rpm sensor. The calibration procedure for the rpm sensor is unfortunately unknown. Another explanation for a deviation is an interference between impeller and guide vane frequency.

The second most dominant frequency is the low frequent 0.6 Hz. This frequency is also present in all the runner transducers. The frequency was found to be independent of turbine rotation (0.6 Hz found at 180 and 412 rpm). The frequency changed with the water level in pressure tank which indicates an elastic mass oscillation. How this frequency came to be was not discovered.

The last significant frequency is 96.25 Hz and will be discussed in the next section.
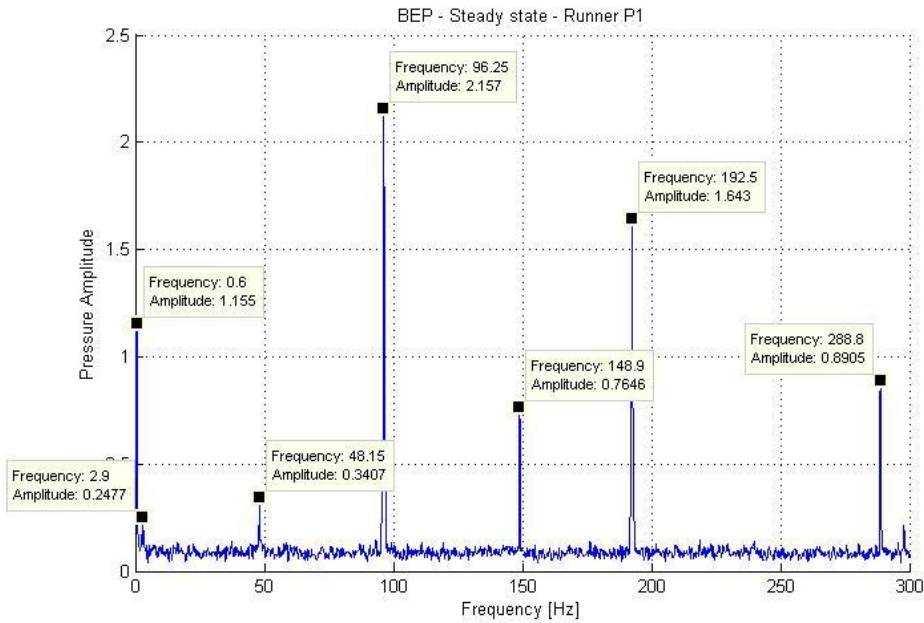
5.3.3 Runner transducers

The biggest amplitude in Figure 5.3-6 is 96.25 Hz with its half (48.15Hz), second (192.5 Hz) and third (288.8) harmony. The fundamental frequency of 96.25 Hz is traceable in all eight transducers for all operational points. The frequency was found to be independent of the runner rotational speed. Control testing confirmed these exact frequencies at 279, 332 and 523 rpm turbine. Figure 5.3-7 shows the amplitudes for 96.3 Hz through the whole system.
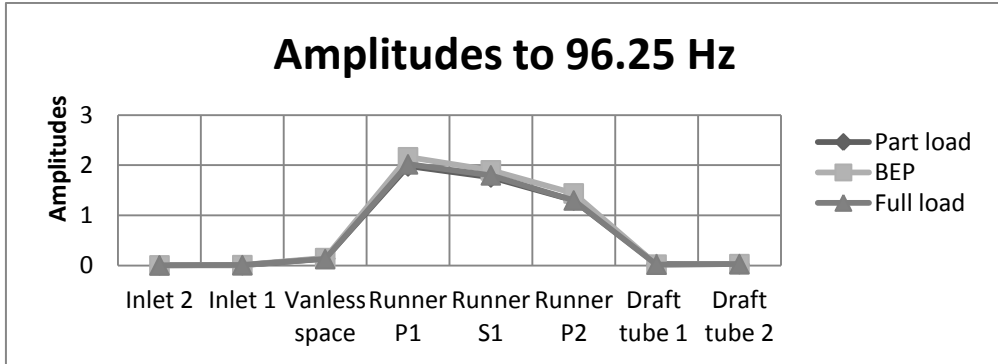
Figure 5.3-7 – Amplitudes for 96.3 Hz for all transducers at three operational points

This frequency is constant for various speeds which imply an elastic fluctuation in the system. The frequency is too high to be u-tube fluctuations. The other considered explanation is the water hammer frequency. The upstream (14.6 m) and downstream (5.6 m) water hammer frequency for various possible speed of sound is presented in Table 5-3. The water hammer definition is found in the theory section 3.2.2 in this report.

Speed of sound[m/s]	Downstream freq [Hz]	Upstream freq [Hz]
700	31.3	12
900	40.2	15.4
1200	53.6	20.5

Table 5-3 – Possible frequencies for water hammer effect.

96.25 Hz is no were near the frequencies presented in Table 5-3. Torbjørn Nielsen suggested a possible overtone phenomenon. This phenomenon was studied and a review of this study was developed and can be seen in appendix E. If one were to consider the possibility of overtone frequencies upstream or downstream to the turbine, the first overtone would be 3 times the fundamental frequency ($3f_{wh}$). One third of 96.3 Hz is 32.1 Hz and would give a speed of sound of 719 m/s which could be reasonable.

This overtone phenomenon could also help explain another elastic oscillation discovered in the draft tube. A similar speed of sound would give an upstream overtone frequency ($3f_{wh}$) that could explain the 38 Hz in Figure 5.3-9.

An unrelated frequency is the 148.9 Hz in Figure 5.3-6. This oscillation was found to be rotational dependent. It was only detected in the runner transducers. During control testing this frequency was found to decrease and

increase along with the turbine rotational speed. The guide vane frequency for BEP is 154.9 Hz. As for the impeller vane frequency in the vaneless space there is a 4% deviation between expected (159.9 Hz) and measured (148.9 Hz) guide vane frequency.

While transducer S1 and P2 always showed traces of the guide vane frequency the P1 transducer did not. In operational points outside BEP, a rotation independent frequency of 144.4 Hz was found for this transducer. Transducer P1 is placed in the middle of the blade (see Figure 5.3-8). One possible explanation could be that this transducers experience the natural or resonant frequency of the turbine runner.
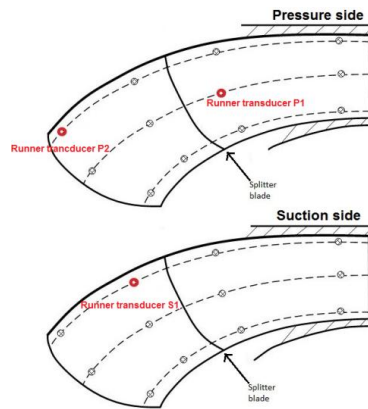
Figure 5.3-8 – Runner transducer placements

5.3.4 **Draft tube transducers**
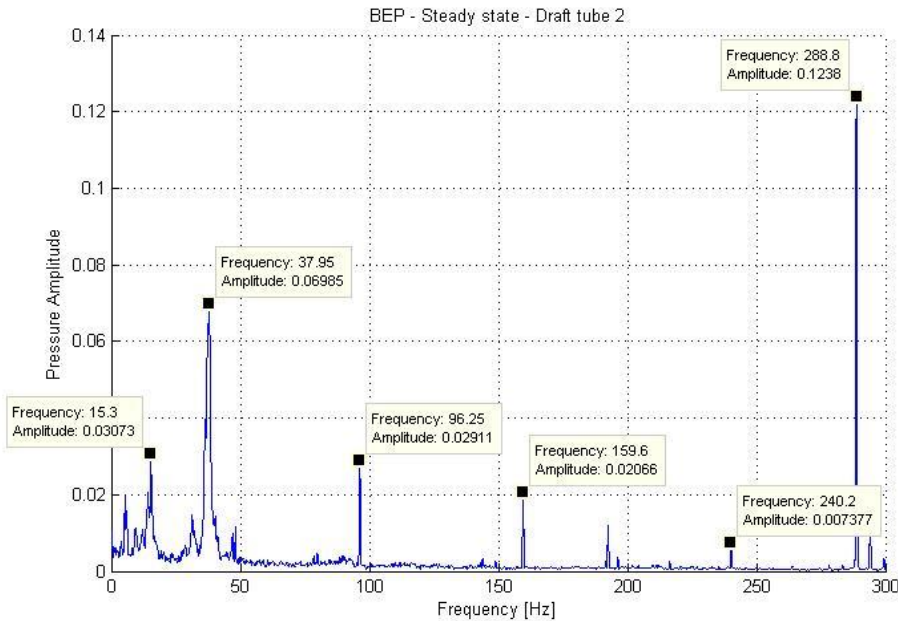
Figure 5.3-9 Steady state – BEP – Frequency domain draft tube transducer 2

The most dominant frequency in Figure 5.3-9 is the 288.8 Hz frequency. This is thought to be the third harmony of 96.25 Hz. Why it is significantly bigger in amplitude than its assumed fundamental frequency (96.25 Hz) is unknown. This occurrence is unique for the draft tube transducer 1 and 2.

Distinct traces of the suspected impeller vane frequency (160 Hz) and its second harmony (240 Hz) is seen in the figure.

The significant amplitude at 38 Hz is mentioned in previous section and the only appraised explanation is the mentioned overtone phenomenon.

It was unsuccessful to find any consistent low frequent oscillations. No Rheingans frequency has been observed trough out the steady state measurements. There was neither any visible evidence of this oscillation in the draft tube. One factor might be the close to atmospheric pressure in the draft tube during the experiments.

5.4 **Start and stop**

The result in this section will be presented in the same way as for the steady state with four areas of interest for BEP. Additional visual presentations for part load and full load can be seen in Appendix A.

In figure 5.4-1 the divided periods (1-9) for BEP is plotted. Results from all eight transducers are plotted in the time domain (80,200 log points and 40 seconds). The turbine rotational speed is also displayed on top.
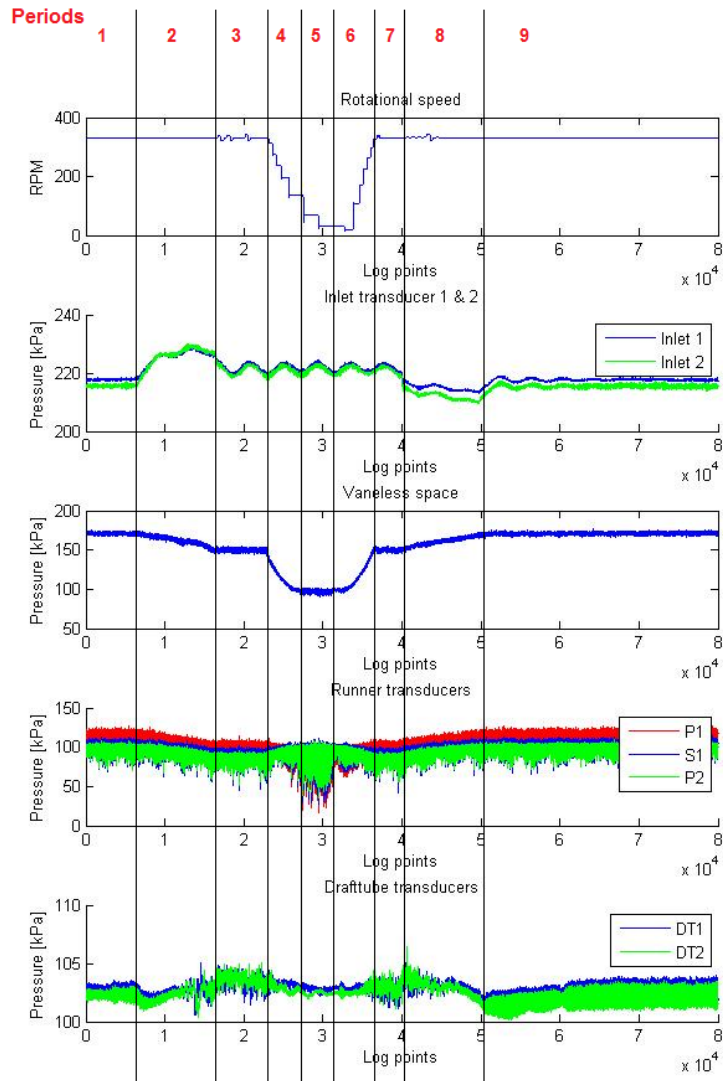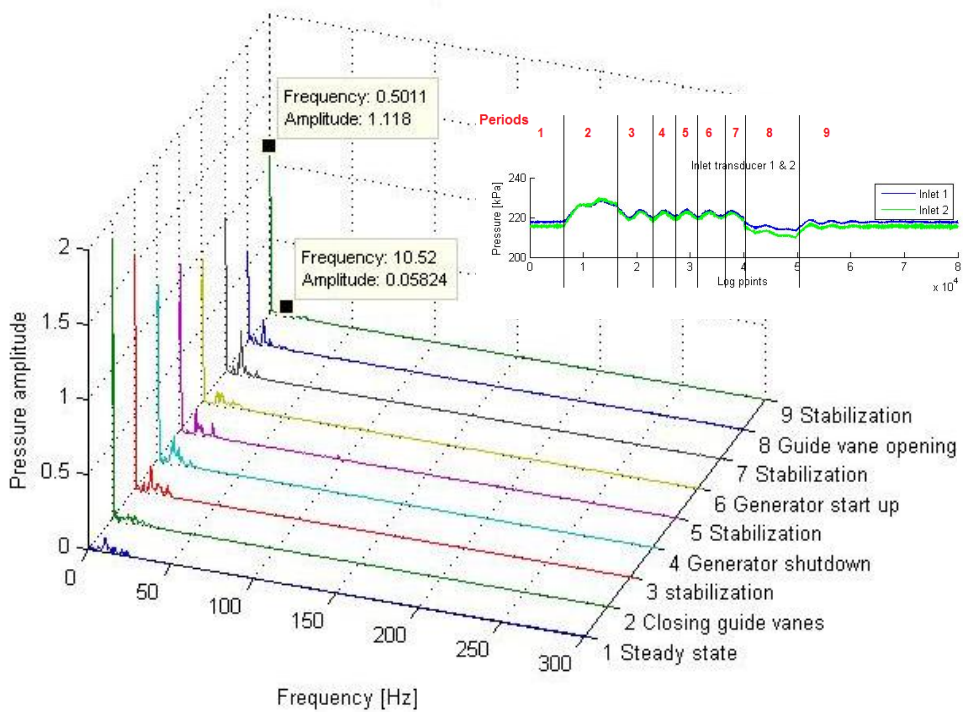

Figure 5.4-1 – Stop start – BEP – Time domain for eight pressure transducers

5.4.1 **Inlet transducers**

Figure 5.4-2 – Stop/Start – BEP –Frequency domain Inlet transducers 1 for 9 periods

From the frequency domain in Figure 5.4-2 one can see relative large amplitudes at 0.5011 Hz from period 2 and throughout the stop and start procedure. This exact frequency was found at all transducers and most periods. When investigated, it was discovered that the frequency changed according to changes in the sampling size. The sampling size for each period is only 2 seconds (4010 log points) and this could have been a problem for the current Matlab script. Low frequencies (under 1 Hz) cannot be considered as exact frequencies. However, the amplitudes for the low frequencies do in fact reflect the original signal. This can be seen in period 2 when guide vanes are closing and the oscillation is at its highest.

The frequency at 10 Hz is the unknown rotational dependent frequency discussed in section 5.3.1- steady state.

In the time domain in the figure above one can see the low frequent oscillations stating in period 3 after the guide vanes are closed. Stop/start procedures were conducted on three different water levels in the pressure tank. The water level in the tank was changed between 70, 89 and 100% while the rotational speed was kept constant. The results can be seen in Figure 5.4-3 were the pressure from the inlet transducers are plotted for 50 seconds.
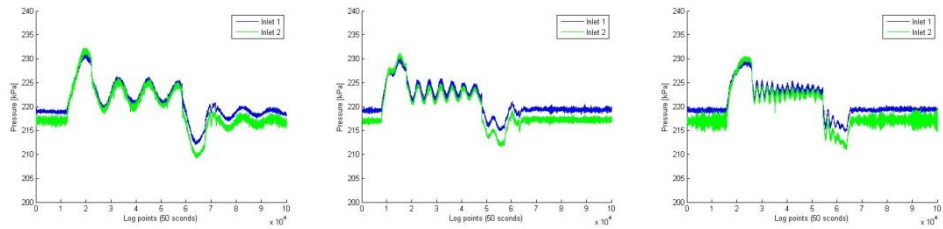
Figure 5.4-3 – Stop/start – n=332 rpm – Inlet transducer 1 & 2 - 70, 89 and 100% water level in pressure tank

The oscillation frequency created by the guide vane closing increases drastically with occupancy level in pressure tank.

5.4.2 **Vaneless space transducer**
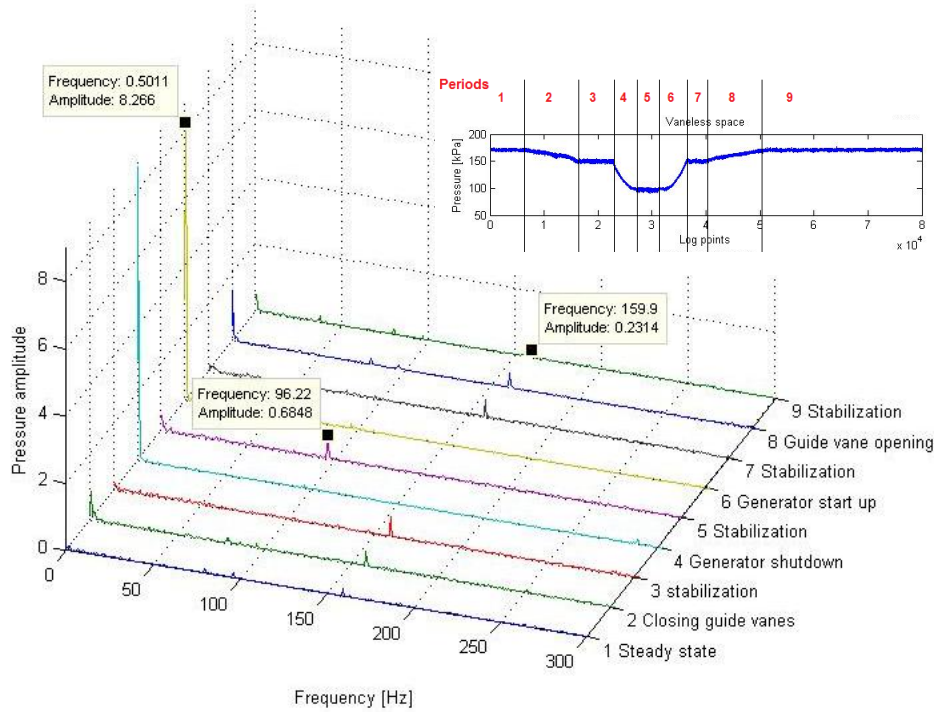
Figure 5.4-4 - Stop/Start – BEP –Frequency domain Vaneless space transducers for 9 periods

As discussed in the previous section the low frequent oscillations cannot be considered to be exact, but the large amplitudes in period 4 and 6 corresponds well to the time domain and its significant fluctuations.

The impeller frequency (159.9 Hz) is present for 6 periods and naturally it disappears when the rotational speed changes. Figure 5.4-5 displays the amplitudes for the impeller vane frequency through the stop/start procedures.
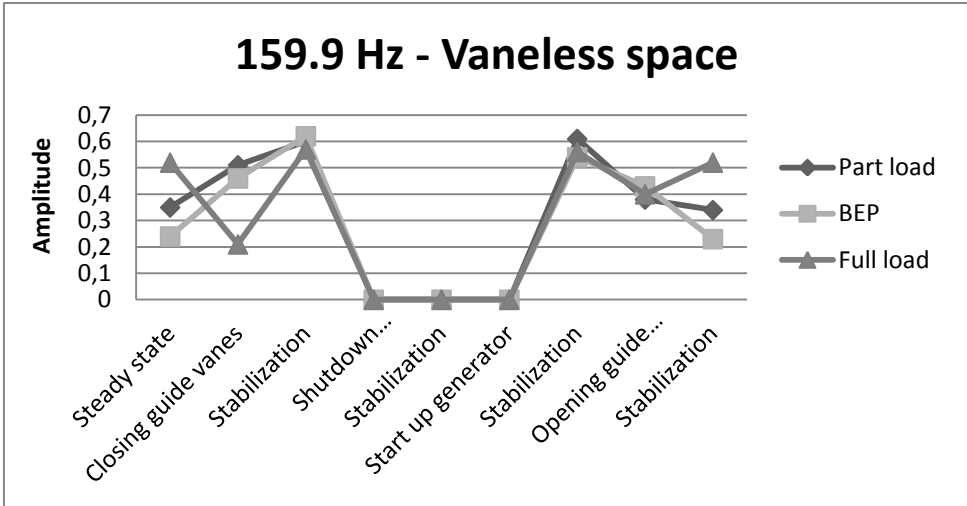
Figure 5.4-5 –Amplitudes for impeller vane frequency during stop/start in vaneless space

The amplitude for the impeller vane frequency does almost triple in size during guide vane closing for BEP. The amplitude increase for part load and full load are less significant.
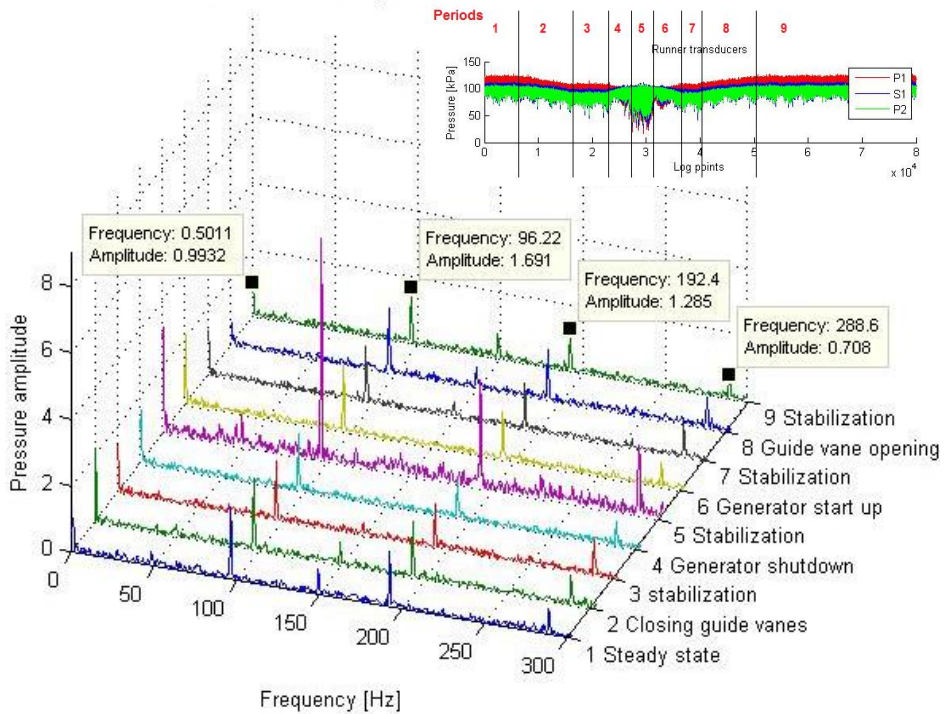
5.4.3 **Runner transducers**

Figure 5.4-6 – Stop/Start – BEP –Frequency domain Runner transducer P1 for 9 periods

The highest amplitudes during measurements were found in the runner. This is seen of Figure 5.4-6. The most dominant frequency is the 96.22 Hz which was discussed in section 5.3.3. The two higher frequencies at 192.4 and 288.6 Hz is most likely the second and third harmonic to this fundamental frequency. In Figure 5.4-7 the amplitudes for this frequency can be seen for the three runner transducers. It is worth noting that the amplitudes do not increase during opening or closing of the guide vanes.
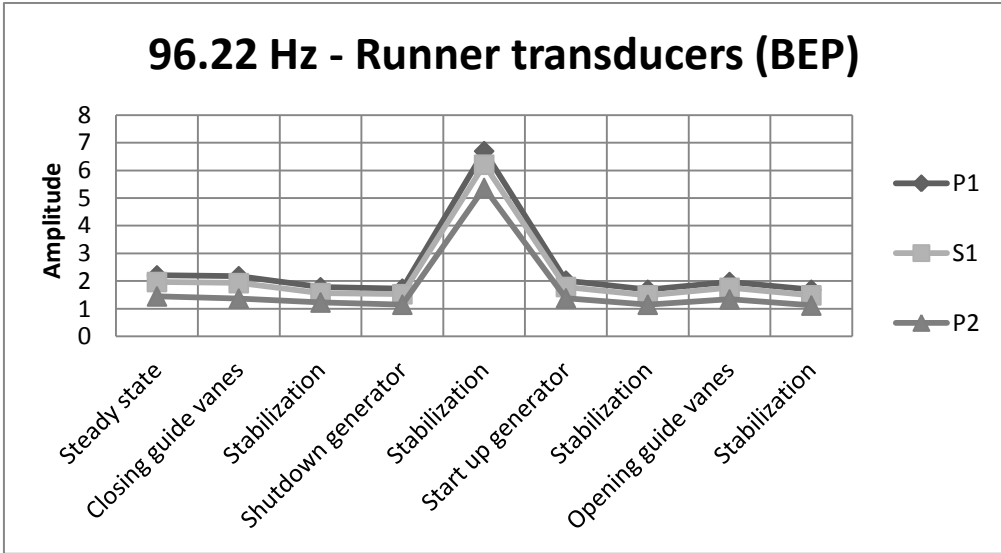
Figure 5.4-7 – Amplitudes at 96.22 Hz for runner transducers at BEP

After the generator is shutdown and the runner is slowing down, the amplitude for the 96.22 Hz frequency increases significantly.

Another high frequency which can be seen on Figure 5.4-6 is 148.8 Hz. This particular frequency was also discussed in the steady state section (5.3.3) of this report. A possible explanation for this oscillation is the guide vane frequency. This frequency is only seen on the three runner transducer and decreases during closing of the guide vanes as seen in Figure 5.4-8. No visible amplitudes for period 4, 5 and 6.
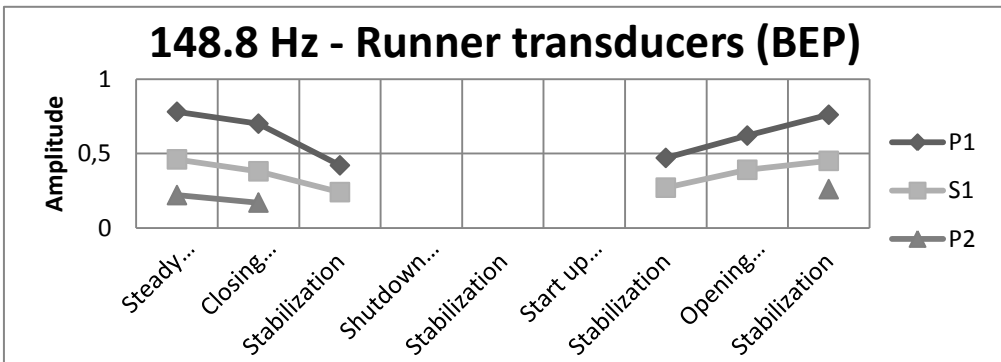
Figure 5.4-8 - Amplitudes at 148.8 Hz for runner transducers at BEP
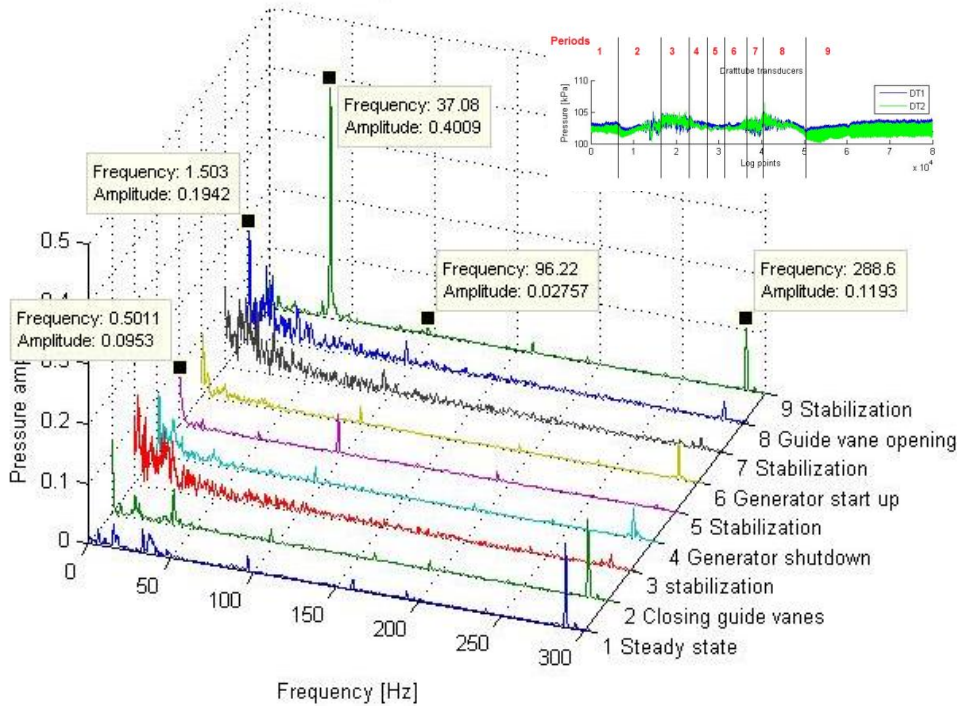
5.4.4 **Draft tube**

Figure 5.4-9 - Stop/Start – BEP –Frequency draft tube transducer 1 for 9 periods

Most of the low frequent oscillations in the draft tube during stop/start are very difficult to pin point due to large amount of spectral noise. In period 7 there is relatively large amplitude for 1.5 Hz. This frequency does match the Rheingans frequency which would be somewhere in the range of 1.3 to 1.8 Hz.

The amplitude at 37.1 Hz is seen as the most dominant. This frequency is not present when the guide vanes are closed. This could suggest the overtone phenomenon (discussed in section 5.3.3) where this frequency would be a water hammer oscillation to the upstream water column.

The frequency of 288.6 Hz is a rotational independent frequency. It dampens when the guide vanes are closed and until guide vanes are fully open. In Figure 5.4-9 one can also see that when the amplitudes of 288.6 Hz decrease, the amplitude of 96.22 Hz increases.

42

6. **Conclusion**

The impeller vane frequency is the dominant oscillation in the vaneless space. Frequency analysis shows a large amplitude increase during guide vane closing for best efficiency point (BEP). Results indicate a bigger amplitude increase for BEP than for other operational points. Minor traces of the impeller vane oscillation were found in the draft tube.

The guide vane frequency was located in the runner. The amplitude of the guide vane frequency was significant and was located for all studied operational points. The power of this oscillation decreases during guide vane closing.

The most dominant frequency in the runner was found for a rotational independent frequency (96 Hz). Traces of this frequency were also detected in the inlet, vaneless space and draft tube.

Another significant rotational independent frequency was discovered inside the runner for operational points outside BEP. This oscillation had a frequency of 144.4 Hz and was only evident for one of the three runner transducers.

Traces of the Rheingans frequency was not confirmed for any of the various operational points. No visible vortex was seen in the transparent draft tube.

7. **Further work**

Measure the actual speed of sound for the Waterpower laboratory. With this parameter known, the overtone phenomenon could be more accurately studied. This would also be highly advantageous to help identifying the water hammer frequency.

To be able to pin point low frequent oscillations during start and stop, a different method for frequency analysis could be explored. The Joint Time-Frequency Analysis (JTFA) is one possible tool to try for the transient signals.

8. **Bibliography**

Bakken, B.H., et al. 2001. *Start/stopp-kostnader for vannkraftverk.* Trondheim : SINTEF, 2001. 82-594-1980-7.

Dahlhaug, Ole Gunnar. 2007. *Tokke model test 2006-2007 NTNU reference runner.* Vannkraftlaboratoriet, Trondheim : NTNU, 2007.

Gidskehaug, Sindre Lavik. 2010. *Trykkpulsasjoner i Francisturbin.* Trondheim : NTNU, 2010.

Goldman, Steve. 1999. *Vibration Spectrum Analysis: A practical approach.* s.l. : Industrial Press Inc, 1999. 0831130881.

Guttormsen, Odd. 2006. Kompendium TVM4165 Vannkraftverk og vassdragsteknikk. Trondheim : SIT-Tapir, 2006.

Haugan, Kari. 2007. *Trykkpulsasjoer i francisturbiner.* Trondheim : NTNU, 2007. EPT-M-2007-20.

Haugen, J. O. 1994. *Laboratoriet - Typiske frekvenser i strømningsmaskiner.* s.l. : Inernt notat fra GE Turbinlaboratoriet, 1994.

IEC, Ineternational Electrotechnical commission. 1999. *IEC 60193 - Hydraulic turbines, storage pumps and pump-turbines - model accepance tests.* s.l. : Ineternational Electrotechnical commission IEC , 1999. CEI/IEC 60193:1999.

Kobro, Einar. 2010. *Measurement of pressure pulsation in francis turbines.* Trondheim : Norwegian University of science and technology, 2010. ISBN 978-82-471-2239-6.

—. 2006. *Trykkpulsasjoner i Francisturbiner.* NTNU, Norway : Vannkraftlaboratoriet, 2006.

Moen, Anette Surtevju. 2012. Correspondence with Statkraft employee. . 2012.

National Instruments. jun, 2011. *Transient Recording Using PC-based Instrumentation.* s.l. : National Instruments, jun, 2011.

—. dec, 2011. *Windowing: Optimizing FFTs Using Window functions.* . s.l. : National Instruments, dec, 2011.

Nielsen, Torbjørn K. 1990. *Dynamisk Dimensjonering av vannkraftverk.* Trondheim : NTNU, 1990. ISBN: 82-595-5952-8.

Nielsen, Torbjørn. 2012. Talks. Waterpower laboratory, Trondheim : s.n., 2012.

Physics-classroom. 1996-2012. The Physics Classroom. [Online] comPADRE, 1996-2012. http://www.physicsclassroom.com/.

Rheingans, W. J. 1940. *Power Swings in Hydroelectric power plants* . Milwaukee, Wisconsin : s.n., 1940.

Tørklep, Anders Mathias. 2011. *Pumpeturbins oppførsel i forskjellige driftspunkter.* Trondheim : NTNU, 2011.

Wheeler, Anthony J. and Ganji, Ahmad R. 2010. *Introduction to Engineering Experimentation - third edition.* s.l. : Pearson, 2010. ISBN-10: 0-13-511-314-8.
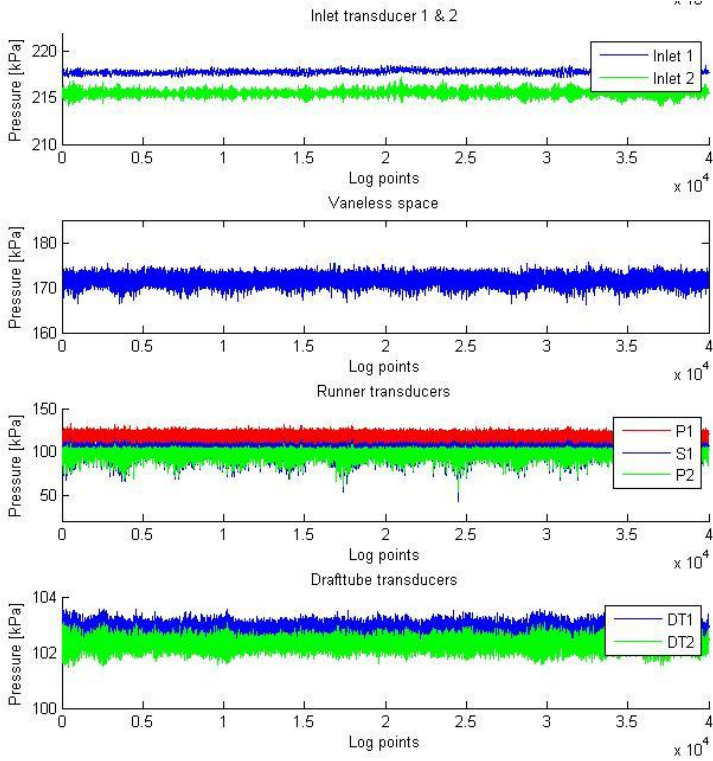
9. **Appendix**

Table of content

Appendix A – Results

Steady state - Part load
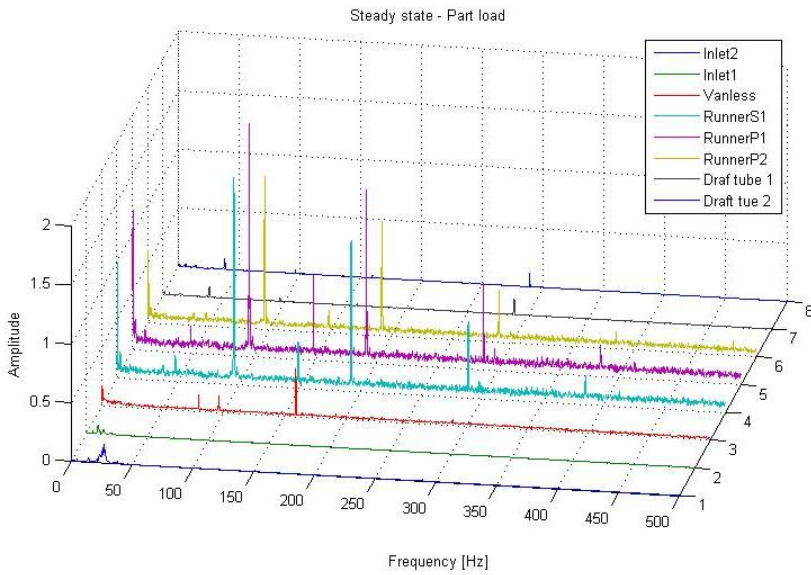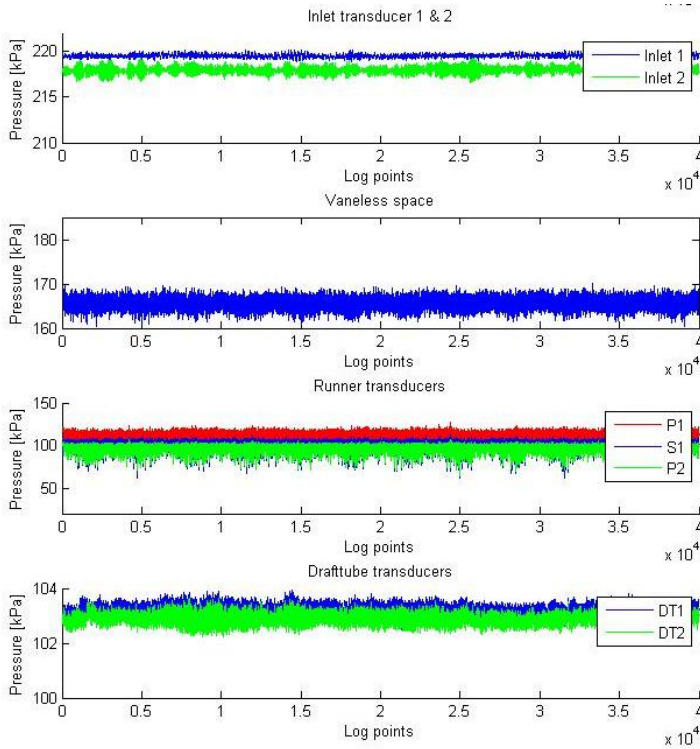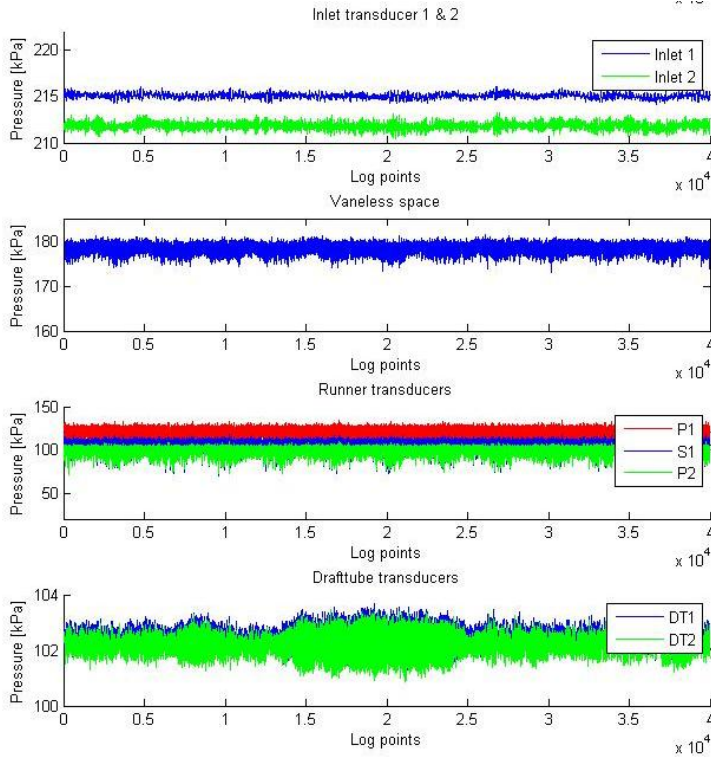
Steady state - BEP
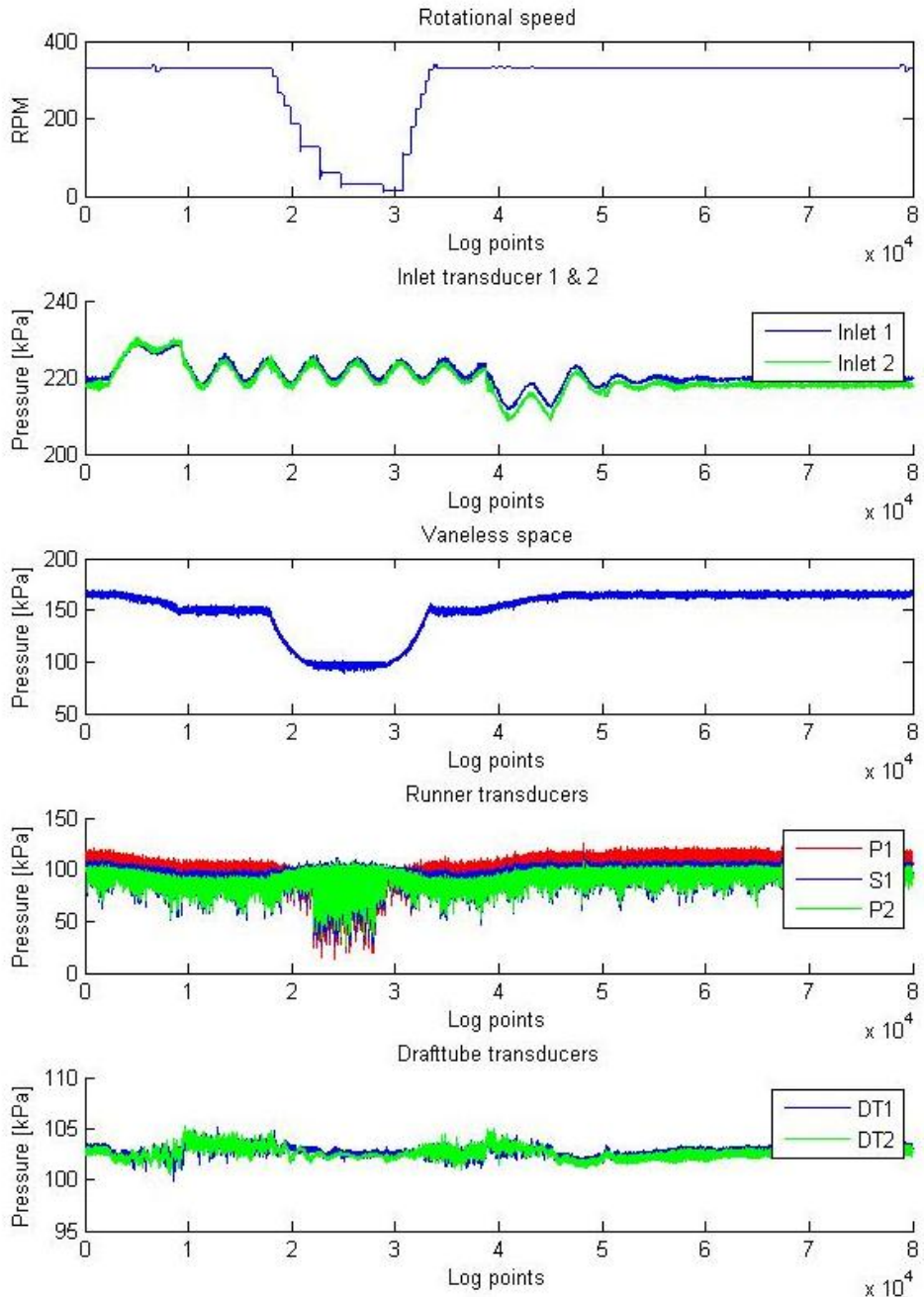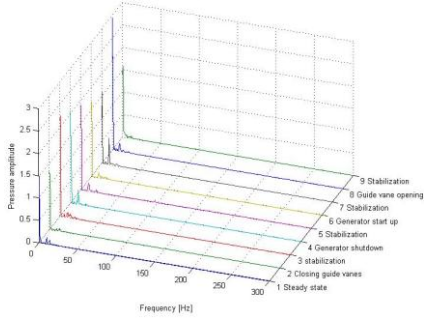
Appendix

Steady state - Full load
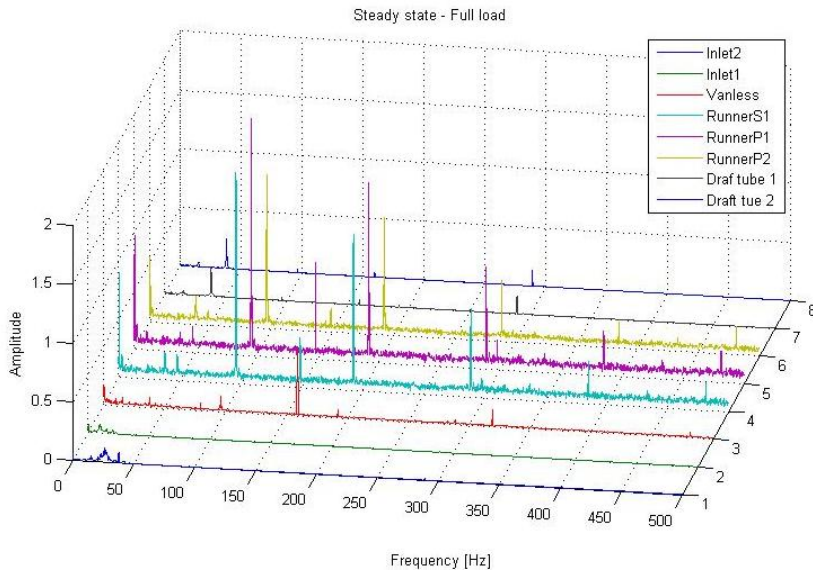
Stop/start – Part load

Shut down and start up in part load operation. 80,000 log points equals 40 seconds.
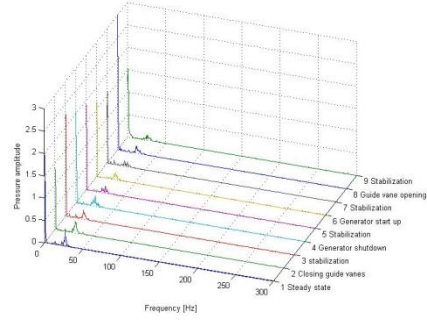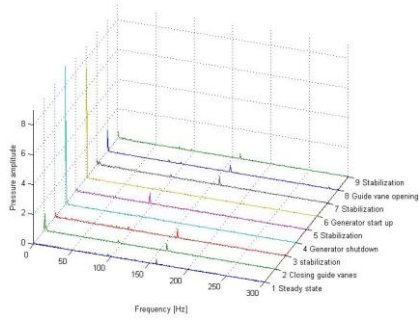
Appendix

Stop/start - BEP

Shut down and start up in BEP operation. 80,000 log points equals 40 seconds.

Appendix

BEP - Stop/start - Inlet 1

BEP - Stop/start - Inlet 2

BEP - Stop/start - Vanless space

BEP - Stop/start - Runner P1

BEP - Stop/start - Runner S1

BEP - Stop/start - Runner P2

BEP - Stop/start - Draft tube 1

BEP - Stop/start - Draft tube 2
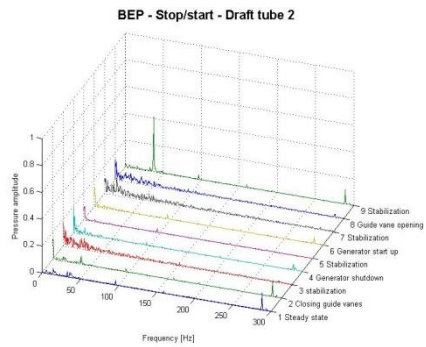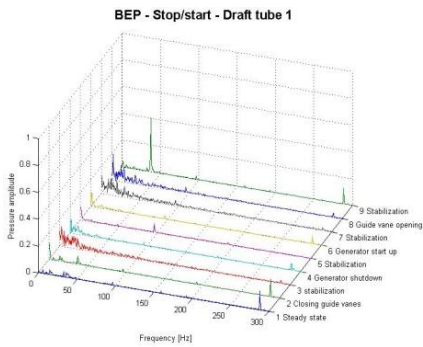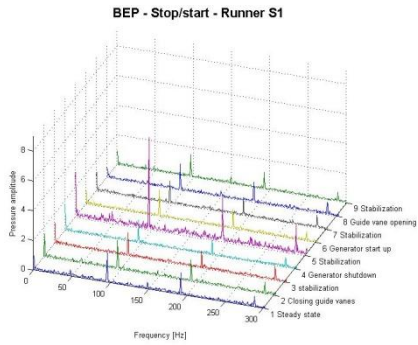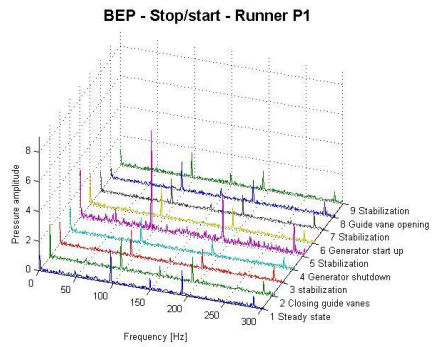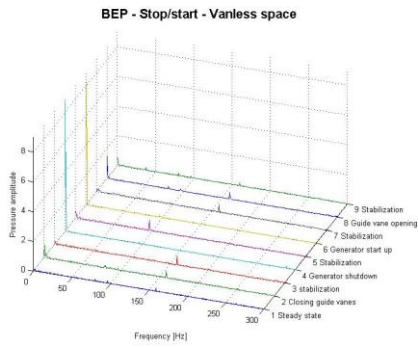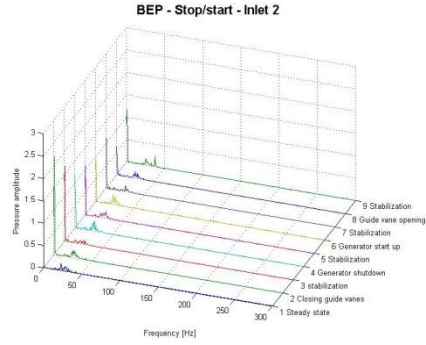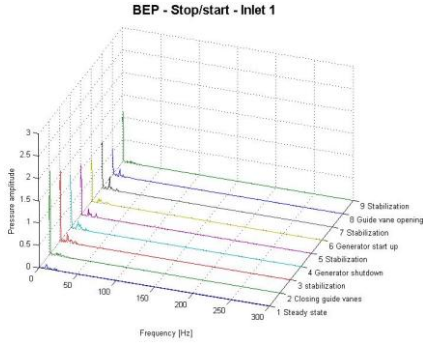
Stop/start - Full load
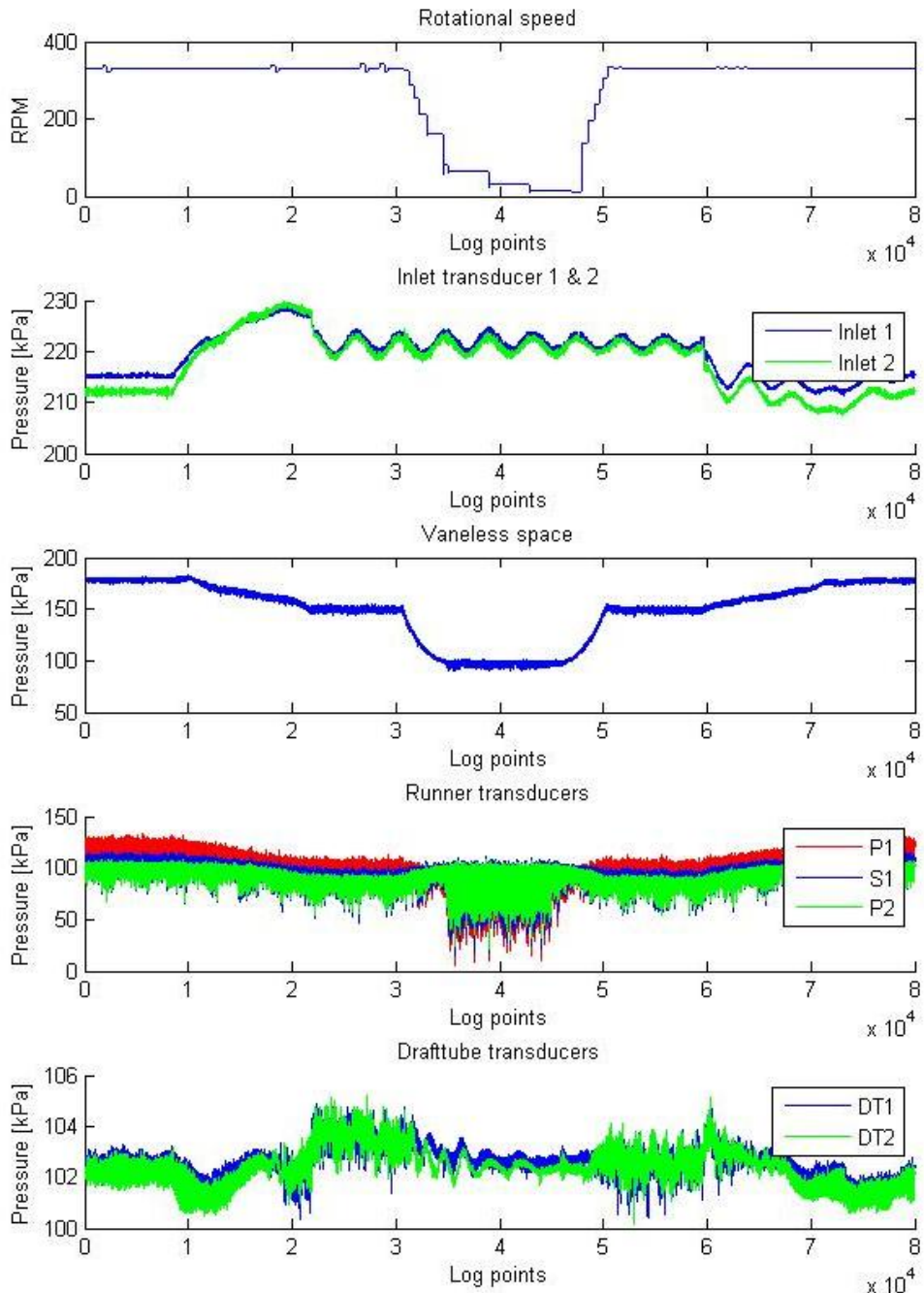
Shut down and start up in full load operation. 80,000 log points equals 40 seconds.
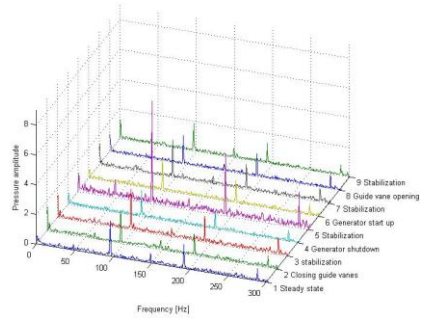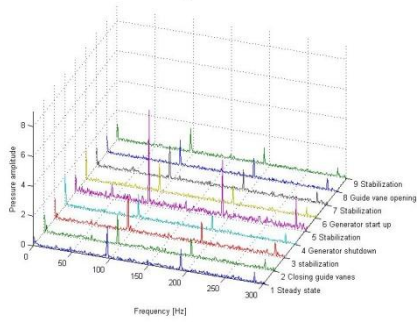
Full load - Stop/start - Inlet 1
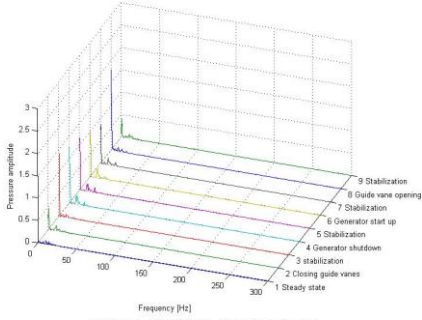
BEP - Stop/start - Inlet 2
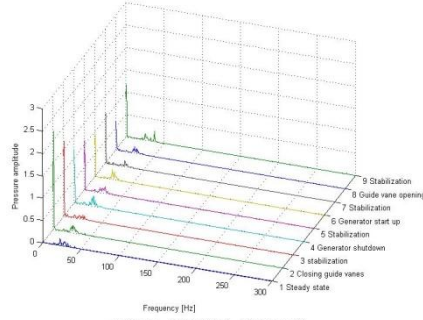
Full load - Stop/start - Vaneless space
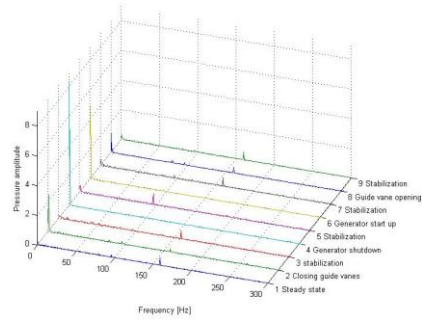
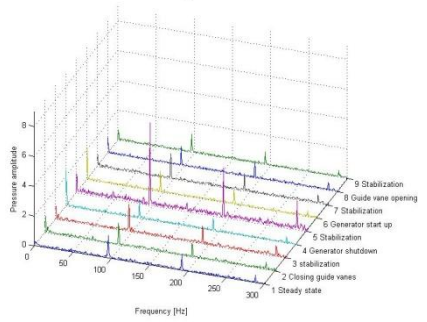Full load - Stop/start - Runner P1
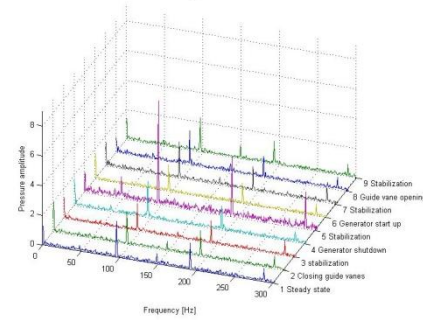
BEP - Stop/start - Runner S1
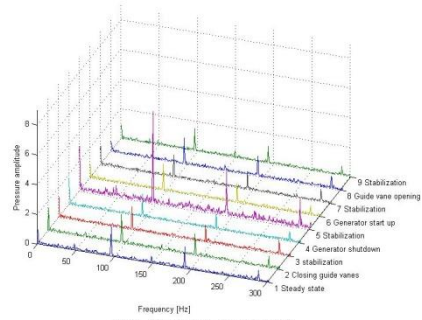
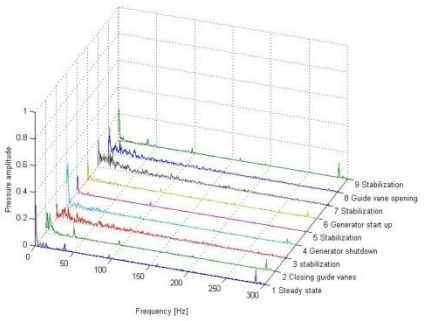BEP - Stop/start - Runner P2
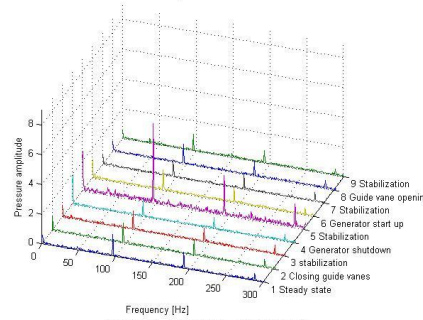
BEP - Stop/start - Draft tube 2
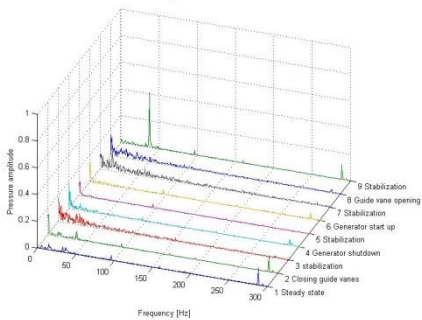
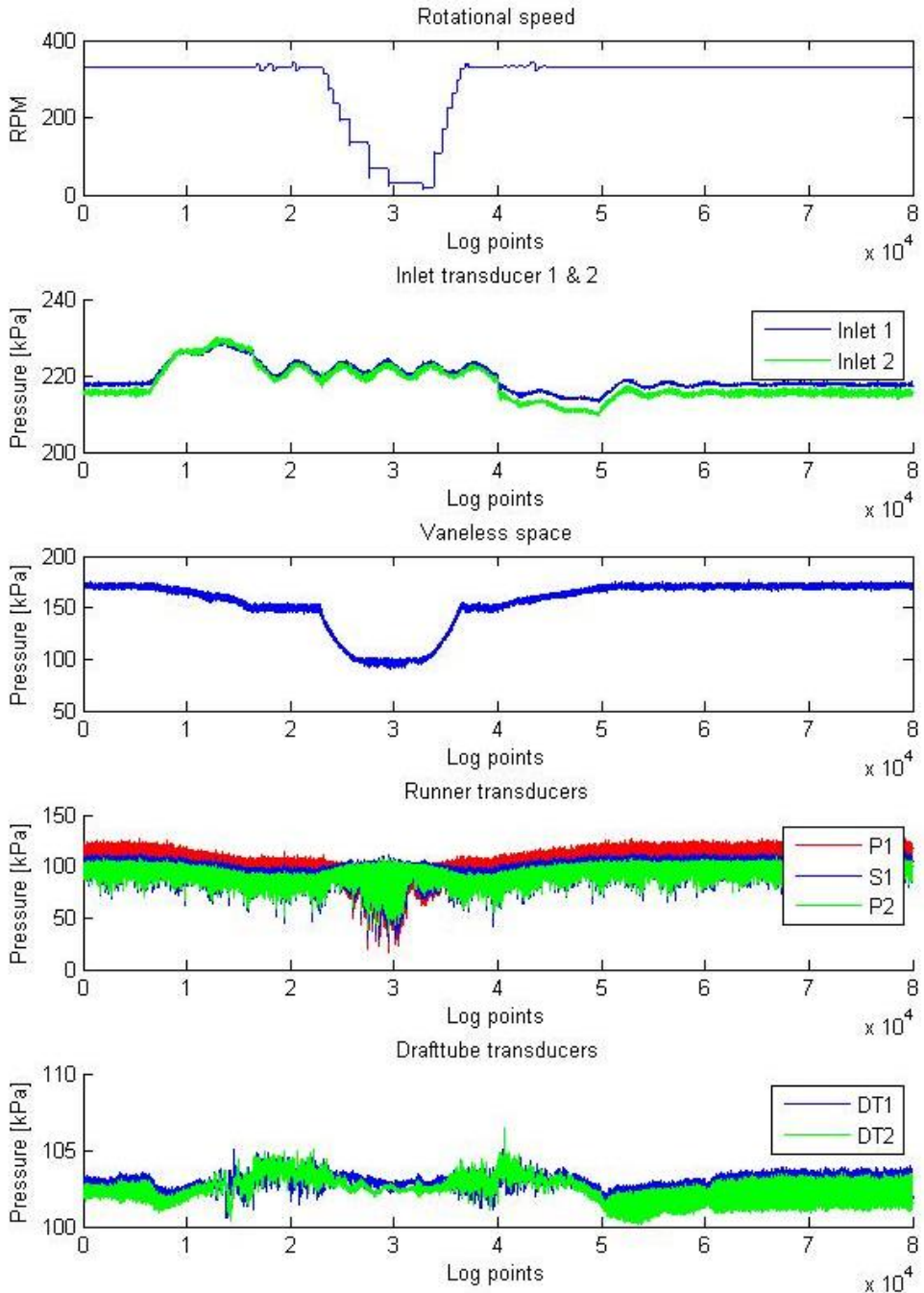Full load - Stop/start - Draft tube 1
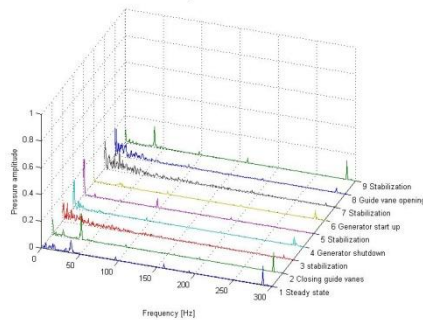
Appendix B Calculations

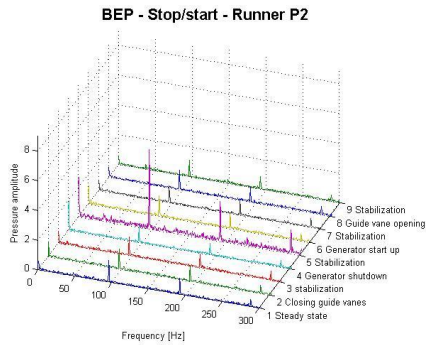All calculations are done with respect to the distance between turbine and pressure tank. The moment of inertia to the turbine was found by drawing the runner in Inventor with following properties:

- Mass: 238 kg
- Volume: 0.027 m^3

Inventor calculated the moment of inertia to I_{zz}=10.6 kgm^2. All other properties and number were found from previous work done on the Tokke model turbine and from the Waterpower laboratory.

Oscillating mass T_A:

$$T_a = J \times \frac{\omega_0^2}{P_{max}} = J \times \frac{(\frac{n\pi}{30})^2}{Q\rho g H \eta}$$

$$= 14.8 kgm^2 \times \frac{(\frac{332\pi}{30})^2}{0.2\frac{m^3}{s} \times 1000\frac{kg}{m^3} \times 9.82\frac{m}{s^2} \times 11.9m \times 0.93} = 0.85s$$

Mass of water T_w to the pressure tank:

$$T_w = \frac{Q}{gH}\sum \frac{l}{A}$$

$$T_w = \frac{0.27\frac{m^3}{s}}{9.82\frac{m}{s^2} \times 12.3\ m} \times 110.5\frac{1}{m} = 0.247\ s$$

The Lengths and areas are approximated from figure B.1 which is created from inventor files available at the Waterpower laboratory.
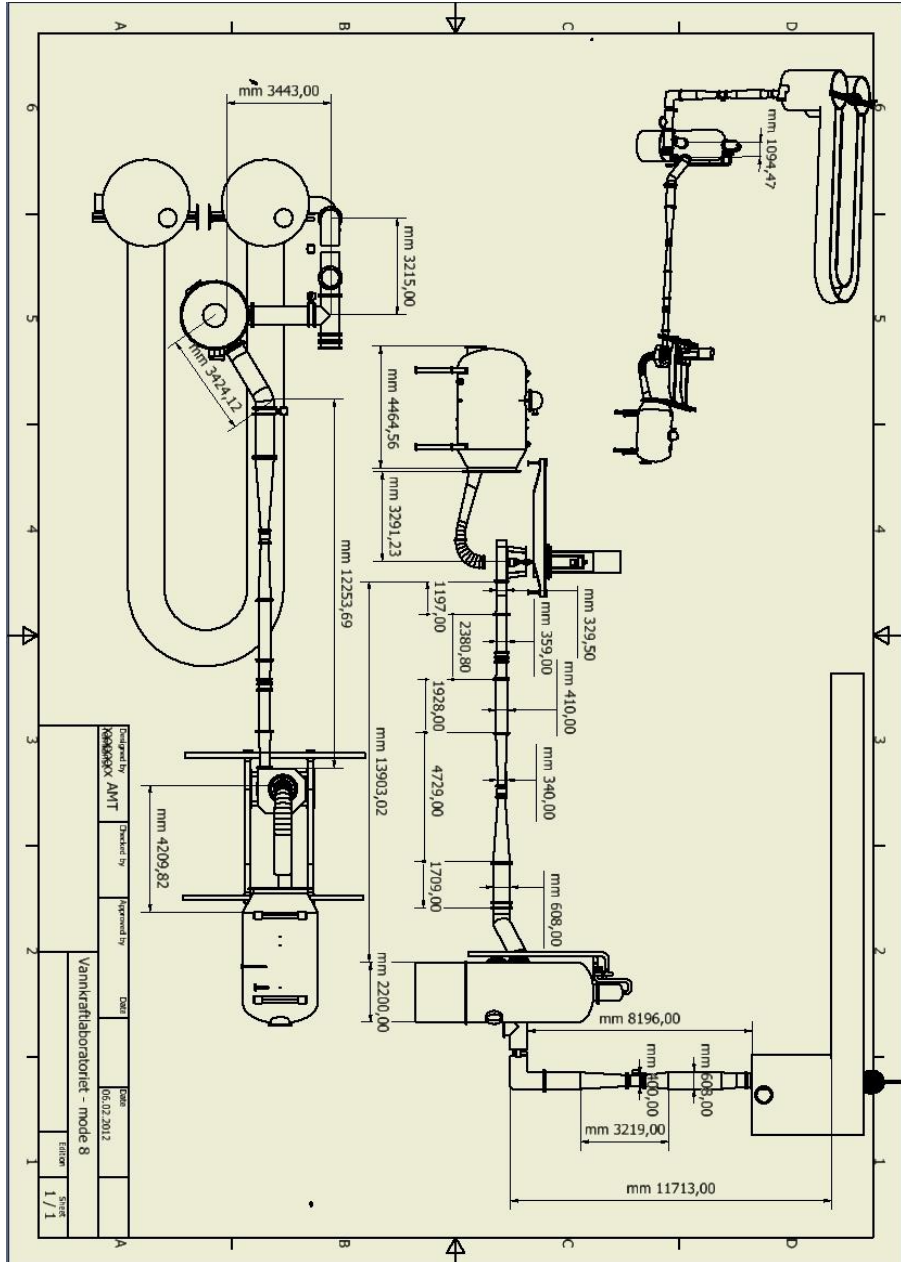
Figure B.1 – Inventor drawing of open loop system at the Waterpower laboratory

Appendix C – Calibration

Every calibration process was conducted at the Waterpower laboratory at NTNU. The inlet transducers were already installed and calibration was conducted on a deadweight tester by PhD candidate Ewe Walseth. Calibration of the draft tube and vaneless space transducers was also carried out on deadweight testers in collaboration with Audun Tovslid. Specifications on the deadweight testers used can be seen in table C-1.

Producer	Type	Model	Accuracy	Range
GE	Hydraulic deadweight tester	P3223-1	0.008%	1-350 bar
GE	Pneumatic deadweight tester	P3023-6-P	0.008%	30-2000 mbar

Table C-1 – deadweight testers used for calibration

The runner transducers had to be calibrated installed on the runner. Therefore a pressure chamber was constructed to calibrate these transducers. An explanation of the procedure and experience gained is as follows: There are mounted 24 pressure transducers in the Tokke runner. According to Einar Kobro (Kobro, 2010), some of the transducer was not working and this was probably due to water leaking inside the sensors. At a later time Joar Grilstad at the waterpower laboratory found 12 sensors to be functional and these 12 were prepared for calibration. The setup for the calibration has been done with the intention of keeping the setup as similar to the actual measurements as possible. The calibration for this system was done with the following equipment:

Hardware	Type	Range	Bandwidth
PC with Labview	National Instruments Labview v11.0	Programmable	50k sampling per second
USB Logging box	National Instruments NI-USB 6211	4-20 mA 2-10V	250k sampling per second
Wireless transmitter	SRI-500e	± 2,5 V	17k sampling per second
Wireless receiver	SRI-500e	± 10 V	Compatible with transmitter

Figure C.1 – utilized calibration equipment.

The whole runner was lower in to a chamber designed by Audun Tovslid. See figure C.2

Figure C.2 Runner installation (left) and overview of calibration setup.

One of the first challenges was to achieve a satisfactory closed system. The designed pressure chamber only showed a minor leakage exposed to 14 bars. Calibration was to be executed for maximum 3 bars and therefore the tightness was found satisfactory. A more significant leak was exposed when extracting the transducer wires through the lid of the pressure chamber. The first wire plug utilized, did show severe leakage at 3 bar a, therefore the plug was changed to the one seen in figure C.3. There was still a leakage, but it was considered to be too small to affect the calibration noteworthy. The leakage was due to water coming out of the inner insulation.
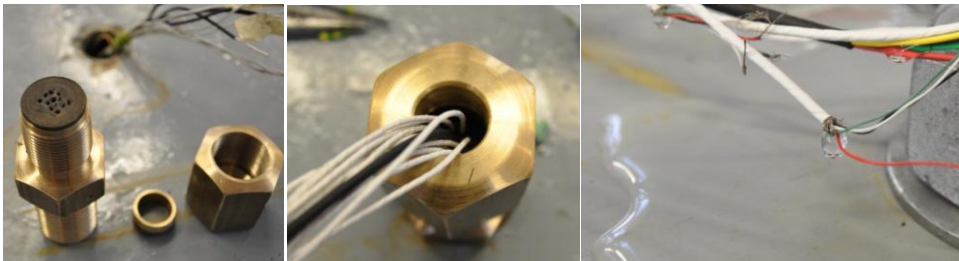
Figure C.3 – The plug and the water leakage through the insulation

Pressure was build up by a hand pump and the pressure inside the chamber was being controlled by a calibrated PTX pressure gauge transducer.

During the calibration it was discovered that only 7 transducers were operating properly. The problem with the other 5 transducers was that during calibration sudden jumps in voltage was registered from the sensors. These jumps occurred suddenly without any external excitation. Because of this the sensors where considered unfitted for the experiments and omitted.

The wireless system used for the calibration and the experiments was the SRI-PMD. Einar kobro (Kobro, 2010) experienced an important limitation in this telemetry system. It could not read more than 4 channels. Even though this was a limitation it meant that one could uphold a 16 bit ADC resolution and a sensor sample rate above 2000 HZ. By using more than 4 channels in the PMD system means reducing either resolution or the sample rate. The collaboration with Luleå University gave the opportunity to use two PMD systems since they possessed a SRI PMD as well. The intention was to use 4 transducers on one system and 3 on another system.

It is important to note that disconnected channels in the wireless transmitter will change its voltage signal according to connected channels. If, as an example, channel 1 is the only channel connected to a sensor which experience pressure variations, channel 2, 3 and so on will show similar voltage variations as channel 1.

Because of unmarked wires there was a need to locate which wire was connected to which transducer. The chosen procedure was to blow compressed air on to the transducers to identify each transducer. During this exercise signal response from 4 of the transducers were lost. Unfortunately there was not found a solution to this problem.

Appendix D – Calibration reports

Draft tube transducer 1

CALIBRATION PROPERTIES
Calibrated by: Audun Tovslid & Anders Tørklep
Type/Producer: Kulite
SN: Z73-94 (4537-34)
Range: 0-7 bar a
Unit: kPa
CALIBRATION SOURCE PROPERTIES
Type/Producer: Pressurements deadweight tester P3023-6-P
SN: 66611
Uncertainty [%]: 0,01
POLY FIT EQUATION:
Y= + 86,21561543E+0X^0 + 18,33862115E+0X^1
CALIBRATION SUMARY:
Max Uncertainty   : 0,049108 [%]
Max Uncertainty   : 0,072660 [kPa]
RSQ   : 0,999997
Calibration points : 12

Draft tube transducer 2

CALIBRATION PROPERTIES
Calibrated by: Audun Tovslid & Anders Tørklep
Type/Producer: Kulite
SN: K76-11 (4537-23)
Range: 0-3,5 bar a
Unit: kPa
CALIBRATION SOURCE PROPERTIES
Type/Producer: Pressurements deadweight tester P3023-6-P
SN: 66611
Uncertainty [%]: 0,01
POLY FIT EQUATION:
Y= + 76,53181949E+0X^0 + 9,17850508E+0X^1
CALIBRATION SUMARY:
Max Uncertainty   : 0,027643 [%]
Max Uncertainty   : 0,038416 [kPa]
RSQ   : 0,999999
Calibration points : 12

Appendix

Vaneless space transducer

CALIBRATION PROPERTIES
Calibrated by: Audun Tovslid & Anders Tørklep
Type/Producer: Kulite
SN: Z73-92 (4537-33)
Range: 0-7bar a
Unit: kPa
CALIBRATION SOURCE PROPERTIES
Type/Producer: Pressurements deadweight tester P3223-1
SN: 66256
Uncertainty [%]: 0,01
POLY FIT EQUATION:
Y= + 202,59051050E+0X^0 + 20,12948496E+0X^1
CALIBRATION SUMARY:
Max Uncertainty   : 0,160085 [%]
Max Uncertainty   : 0,336944 [kPa]
RSQ   : 1,000000
Calibration points : 17

Inlet transducer 1

CALIBRATION PROPERTIES
Calibrated by: Eve Walseth
Type/Producer: Druck PTX 610
SN: 2738458
Range: 0-2.5 bar a
Unit: kPa
CALIBRATION SOURCE PROPERTIES
Type/Producer: Pressurements deadweight tester P3023-6-P
SN: 66611
Uncertainty [%]: 0,01
POLY FIT EQUATION:
Y= -62.52598159E+0X^0 + 31.25865615E+0X^1
CALIBRATION SUMARY:
Max Uncertainty   : 0.024921 [%]
Max Uncertainty   : 0.027135 [kPa]
RSQ   : 0.999999
Calibration points : 32

Appendix

Inlet transducer 2

CALIBRATION PROPERTIES
Calibrated by: Eve Walseth
Type/Producer: Druck PTX 610
SN: 2480173
Range: 0-2.5 bar a
Unit: kPa
CALIBRATION SOURCE PROPERTIES
Type/Producer: Pressurements deadweight tester P3023-6-P
SN: 66611
Uncertainty [%]: 0,01
POLY FIT EQUATION:
Y= -62.41171537E+0X^0 + 31.23304831E+0X^1
CALIBRATION SUMARY:
Max Uncertainty   : 0.034157 [%]
Max Uncertainty   : 0.035125 [kPa]
RSQ   : 1.000000
Calibration points : 64

Runner transducer P1

CALIBRATION PROPERTIES
Calibrated by: Chirag, Anders, Audun
Type/Producer: Kulite LL080
SN: sensor 7
Range: 0-3.5 bar a
Unit: kPa
CALIBRATION SOURCE PROPERTIES
Type/Producer: Pressure chamber with Druck PTX1400 ref pressure
SN: -
Uncertainty [%]: 0,01
POLY FIT EQUATION:
Y= + 11.17288577E+0X^0 + 30.83381610E+0X^1
CALIBRATION SUMARY:
Max Uncertainty   : 0.624352 [%]
Max Uncertainty   : 0.680329 [kPa]
RSQ   : 0.999877
Calibration points : 18

Runner transducer P2

CALIBRATION PROPERTIES
Calibrated by: Chirag, Anders, Audun
Type/Producer: Kulite LL080
SN: sensor 8
Range: 0-3.5 bar a
Unit: kPa
CALIBRATION SOURCE PROPERTIES
Type/Producer: Pressure chamber with Druck PTX1400 ref pressure
SN: -
Uncertainty [%]: 0,01
POLY FIT EQUATION:
$Y= + 2.32203159E+0X^0 + 30.38541133E+0X^1$
CALIBRATION SUMARY:
Max Uncertainty   : 0.449300 [%]
Max Uncertainty   : 0.482328 [kPa]
RSQ   : 0.999937
Calibration points : 18

Runner transducer S1

CALIBRATION PROPERTIES
Calibrated by: Chirag, Anders, Audun
Type/Producer: Kulite ll080
SN: sensor 1
Range: 0-10 bar g
Unit: kPa
CALIBRATION SOURCE PROPERTIES
Type/Producer: Pressure chamber with Druck PTX1400 ref pressure
SN:
Uncertainty [%]: 0,01
POLY FIT EQUATION:
$Y= + 19.47106120E+0X^0 + 31.25021319E+0X^1$
CALIBRATION SUMARY:
Max Uncertainty   : 0.226600 [%]
Max Uncertainty   : 0.235303 [kPa]
RSQ   : 0.999986
Calibration points : 20

Full calibration reports with all calibration points are available at NTNU and the Waterpower laboratory.

Appendix E – Standing wave

Pressure oscillations with respect to elastic fluctuations are mechanical standing waves. Therefore it is in order to define a standing wave and more importantly how it is related to frequencies. The theory in this section is gathered from the internet website physics classroom and talks with Professor Torbjørn Nielsen (Nielsen, 2012).

Pressure oscillation in a waterway can occur as resonance vibrations and create a standing wave. A standing wave is merely a wave that remains in a constant position. Figure 5.4-1 shows a standing wave which means the nodes and anti nodes are in a fixed position.
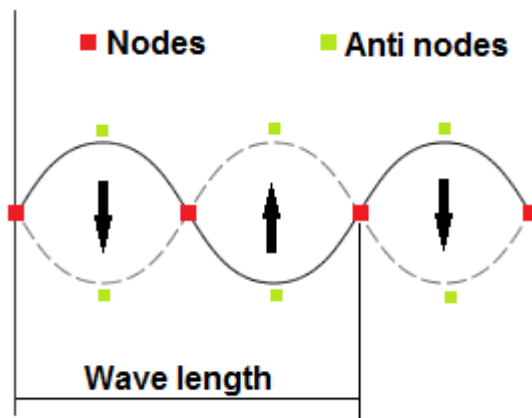
Figure 5.4-1

For resonance vibration in pipes, a standing wave basically has three different ways to behave. Figure 5.4-2 shows the lowest possible frequency for three different cylindrical pipes. The closed ends will behave as nodes while the open ends will behave as antinodes.

Appendix
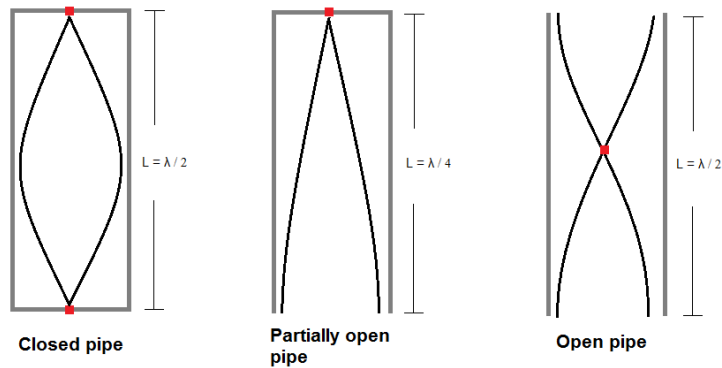
Figure 5.4-2

λ=wave length[m]

In a hydropower plant these alternatives can represent different parts of the whole system. The partially open pipe can represent the water column from the turbine (closed end) to the closest water surface (open end).

By taken a closer look to the partially open pipe there are additional alternatives with respect to the amount of wave cycles. Figure 5.4-3 shows the three lowest possible frequencies for a partially open pipe.
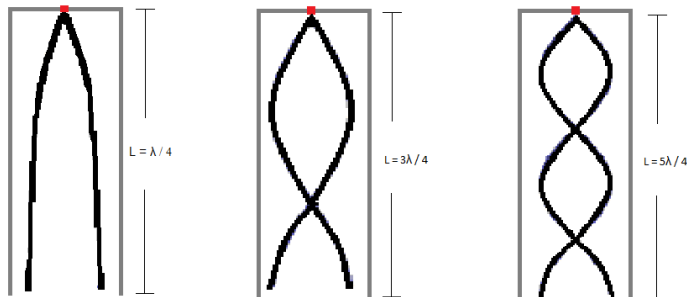
Figure 5.4-3

λ=wave length[m]

The alternative to the left is the fundamental frequency while the two on the right are called overtones. An overtone is in fact a harmony of the fundamental frequency. The fundamental frequency for the partially open pipe will be:

Appendix

Equation 9-1

$$f = \frac{v}{4L}$$

f=frequency [Hz]   v = speed [m/s]   L=length[m]

Note that this equation is equal to what Torbjørn Nielsen used in his definition of water hammer frequency (Nielsen, 1990) and can be seen in Equation 3-6 in this report.

For the first overtone, were the length of the pipe is three quarters of the wavelength (L=3λ/4), the frequency will be:

Equation 9-2

$$f_{O1} = \frac{v}{\lambda} = \frac{3v}{4L} = 3f$$

λ=wave length[m]

This concludes that the first overtone frequency for partially open pipe is the third harmonic of the fundamental frequency.

(Physics-classroom, 1996-2012)

APPENDIX F – Scripts

Matlab script utilized for frequency analysis.

```matlab
clear all
infile1=load('M:\skole\Master\testing\15.05.12\...\9.8deg332.txt');
infile1=infile1(:,8); %The chosen column

nfft=length(infile1);

x1= length(infile1)/2+1;
for i=1:x1
    i1(i)=1;
end
i1=i1';

Fs = 2005;  %logging frequency
window=516*16;  %Size of the window function
overlap_percent=80;
weighting_window=hanning(window);
overlap=floor(0.01*overlap_percent*window);
norm_factor=((norm(weighting_window)^2)/(sum(weighting_window)^2));
[pxx1,f1] = psd(infile1,nfft,Fs,weighting_window,overlap,'mean');

pxx_norm1=pxx1*norm_factor;
pxx_norm1=sqrt(pxx_norm1)*2/sqrt(2);

h=10000;    %Half of logging series
%f1=f1/f;   %Realtive frequency
f1=f1(1:h);
i1=i1(1:h);
pxx_norm1=pxx_norm1(1:h);

figure(2); clf; hold on;  %Time domain
plot(infile1)
xlabel('Time')
zlabel('Pressure [kPa]')

figure(1); clf; hold on;     %Frequency domian
plot3(f1,i1,pxx_norm1);
grid on
xlabel('Frequency [Hz]')
zlabel('Pressure Amplitude')
AZ=0; EL=0;
axis([0 200 1 3]);
grid on;view(AZ,EL)

rms1=sqrt(sum(infile1.*conj(infile1))/size(infile1,1));  % Root mean
square
rms2=sqrt(sum(infile1.*conj(infile1)));
```

Labview program utilized for logging pressure measurements.
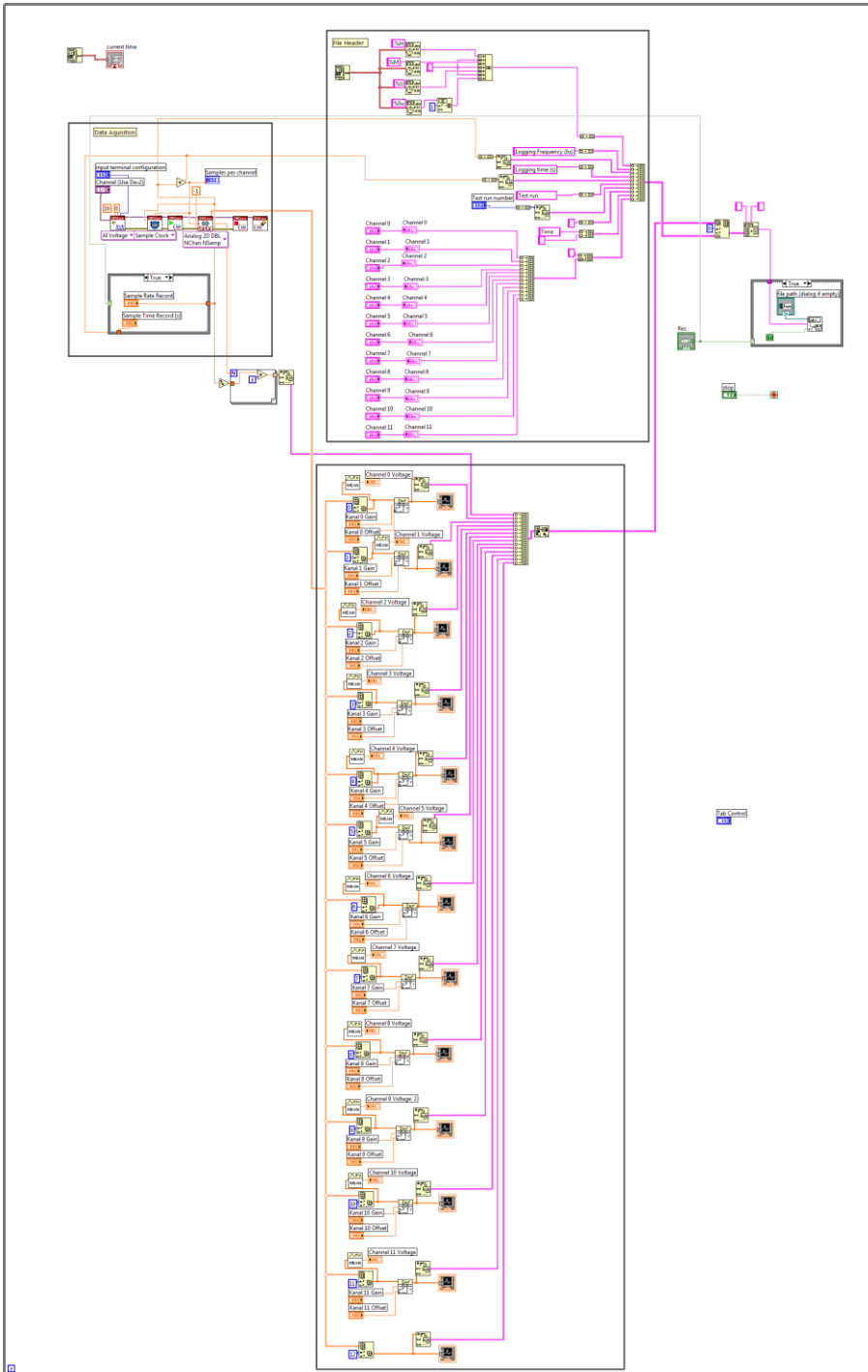
Appendix G – Risk assessment

The risk assessment is done in collaboration with Bård Brandstø at the Waterpower Laboratory at NTNU. There are no incidents concerning health, Safety or Environment (HSE) to report from the laboratory work. A complete risk assessment follows. The repot is written in Norwegian.

Risikovurderingsrapport

Francisrigg; Reversibel Pumpeturbin(RPT)

Prosjekttittel	Modeltest of RPT
Prosjektleder	Torbjørn Nielsen
Enhet	NTNU
HMS-koordinator	Bård Brandåstrø
Linjeleder	Ole Gunnar Dahlhaug
Riggnavn	Demorigg; Francis Rigg
Plassering	Vannkraftlab
Romnummer	42
Riggansvarlig	Grunde Olimstad
Risikovurdering utført av	Grunde Olimstad

INNHOLDSFORTEGNELSE

1   INNLEDNING

Riggen står i hovedrommet til vannkraftlaboratoriet. Formålet med riggen er å gjøre modeltester på løpehjul av typen Francis eller pumpeturbin. Riggen har vært i bruk i lang tid. De aktuelle målingene skal vise virkningsgradsdiagram og karakteristikker for turbinen.

2   ORGANISERING

Rolle	NTNU	Sintef
Lab Ansvarlig:	Morten Grønli	Harald Mæhlum
Linjeleder:	Olav Bolland	Mona J. Mølnvik
HMS ansvarlig:	Olav Bolland	Mona J. Mølnvik
HMS koordinator	Erik Langørgen	Harald Mæhlum
HMS koordinator	Bård Brandåstrø	
Romansvarlig:	Bård Brandåstrø	
Prosjekt leder:	Torbjørn Nielsen	
Ansvarlig riggoperatører:	Grunde Olimstad	

3   RISIKOSTYRING AV PROSJEKTET

Hovedaktiviteter risikostyring	Nødvendige tiltak, dokumentasjon	DTG
Prosjekt initiering	Prosjekt initiering mal	X
Veiledningsmøte	Skjema for Veiledningsmøte med pre-risikovurdering	X
Innledende risikovurdering	Fareidentifikasjon – HAZID Skjema grovanalyse	X
Vurdering av teknisk sikkerhet	Prosess-HAZOP Tekniske dokumentasjoner	X
Vurdering av operasjonell sikkerhet	Prosedyre-HAZOP Opplæringsplan for operatører	
Sluttvurdering, kvalitetssikring	Uavhengig kontroll Utstedelse av apparaturkort Utstedelse av forsøk pågår kort	

4   TEGNINGER, FOTO, BESKRIVELSER AV FORSØKSOPPSETT

Vedlegg:
Prosess og Instrumenterings Diagram, (PID)
Komponentliste med spesifikasjoner
Tegninger og bilder som beskriver forsøksoppsetningen.

5   EVAKUERING FRA FORSØKSOPPSETNINGEN

Se kapittel 14 "Veiledning til rapport mal.
Evakuering skjer på signal fra alarmklokker eller lokale gassalarmstasjon med egen lokal varsling med lyd og lys utenfor aktuelle rom, se 6.2

Evakuering fra rigg området foregår igjennom merkede nødutganger.

6   VARSLING

6.1   Før forsøkskjøring

Varsling per e-post, med opplysning om forsøkskjøringens varighet og involverte til:
- HMS koordinator NTNU/SINTEF
  HaraldStein.S.Mahlum@sintef.no
  Erik.langorgen@ntnu.no
  Baard.brandaastro@ntnu.no
- *Prosjektledere på naborigger varsles for avklaring rundt bruk av avtrekksanlegget uten fare eller forstyrrelser av noen art, se rigg matrise.*

All forsøkskjøringen skal planlegges og legges inn i aktivitetskalender for lab. Forsøksleder må få bekreftelse på at forsøkene er klarert med øvrig labdrift før forsøk kan iverksettes.

6.2   Ved uønskede hendelser

BRANN
Ved brann en ikke selv er i stand til å slukke med rimelige lokalt tilgjengelige slukkemidler, skal nærmeste brannalarm utløses og arealet evakueres raskest mulig. En skal så være tilgjengelig for brannvesen/bygningsvaktmester for å påvise brannsted.
Om mulig varsles så:

NTNU	SINTEF
Labsjef Morten Grønli, tlf: 918 97 515	
HMS: Erik Langørgen, tlf: 91897160	
Instituttleder: Olav Bolland: 91897209	

GASSALARM
Ved gassalarm skal gassflasker stenges umiddelbart og området ventileres. Klarer man ikke innen rimelig tid å få ned nivået på gasskonsentrasjonen så utløses brannalarm og laben evakueres. Dedikert personell og eller brannvesen sjekker så lekkasjested for å fastslå om det er mulig å tette lekkasje og lufte ut området på en forsvarlig måte.
Varslingsrekkefølge som i overstående punkt.

PERSONSKADE
- Førstehjelpsutstyr i Brann/førstehjelpsstasjoner,
- Rop på hjelp,
- Start livreddende førstehjelp
- **Ring 113** hvis det er eller det er tvil om det er alvorlig skade.

ANDRE UØNSKEDE HENDELSER (AVVIK)
NTNU:
Rapporteringsskjema for uønskede hendelser på
 http://www.ntnu.no/hms/2007_Nettsider/HMSRV0401_avvik.doc

7   VURDERING AV TEKNISK SIKKERHET

7.1   Fareidentifikasjon, HAZOP

Se kapittel 14 "Veiledning til rapport mal.
Forsøksoppsetningen deles inn i følgende noder:

Node 1	Rørsystem med pumpe
Node 2	Roterende turbin
Node 3	Hydraulikkanlegg

Vedlegg, skjema: Hazop_mal
Vurdering:
Node1:
-Overtrykksventil som slår ut dersom trykket i systemet blir for høyt.
-Rørelementer er eksternt levert og godkjent for aktuelt trykk.
Node2:
-Roterende utstyr står utilgjengelig for folk. Dvs det er innkapslet eller man må klatre for å nå opp til det.
Node3:
-Trykk i slanger og rør(olje vann) Hydraulikkslanger er ikke egenprodusert
-Trykksatt utstyr er sertifisert og kjøpt inn av eksterne leverandører

7.2   Brannfarlig, reaksjonsfarlig og trykksatt stoff og gass

Se kapittel 14 "Veiledning til rapport mal.
Inneholder forsøkene brannfarlig, reaksjonsfarlig og trykksatt stoff

Ja	Trykksatt hydraulikkolje, trykksatt vann

Vedlegg Ex-sonekart:
Vurdering: *Arbeidsmedium er vann. Alle rør er levert av eksternt firma med prøvesertifikat Hydraulikk til hydrostatisk lager. Hyllevare komponenter, de er dermed ikke egenprodusert.*

7.3   Trykkpåkjent utstyr

Inneholder forsøksoppsetningen trykkpåkjent utstyr:

JA Utstyret trykktestes i henhold til norm og dokumenteres

Trykkutsatt utstyr skal trykktestes med driftstrykk gange faktor 1.4,for utstyr som har usertifiserte sveiser er faktoren 1.8. Trykktesten skal dokumenteres skriftlig hvor fremgangsmåte framgår.
Vedlegg: Prøvesertifikat for trykktesting finnes i labperm.
Vurdering:

7.4   Påvirkning av ytre miljø (utslipp til luft/vann, støy, temperatur, rystelser, lukt)

Se kapittel 14 "Veiledning til rapport mal..

NEI	

Vurdering: Det blir ingen utslipp til ytre miljø.

7.5   Stråling

Se kapittel 14 "Veiledning til rapport mal.

NEI	

Vedlegg:
Vurdering: Ingen strålekilder.

7.6   Bruk og behandling av kjemikalier

Se kapittel 14 "Veiledning til rapport mal.

Ja	

Vedlegg:
Vurdering: Hydraulikkolje, mineralsk olje. Datablad er vedlagt

7.7   El sikkerhet (behov for å avvike fra gjeldende forskrifter og normer)

NEI	

Her forstås montasje og bruk i forhold til normer og forskrifter med tanke på berøringsfare
Vedlegg:
Vurdering: Alt elektrisk utstyr er forsvarlig montert og står slik permanent.

8   VURDERING AV OPERASJONELL SIKKERHET

Sikrer at etablerte prosedyrer dekker alle identifiserte risikoforhold som må håndteres gjennom operasjonelle barrierer og at operatører og teknisk utførende har tilstrekkelig kompetanse.

8.1   Prosedyre HAZOP

Se kapittel 14 "Veiledning til rapport mal.
Metoden er en undersøkelse av operasjonsprosedyrer, og identifiserer årsaker og farekilder for operasjonelle problemer.
Vedlegg: HAZOP_MAL_Prosedyre
Vurdering: Operatør har et eget rom for å kjøre riggen.

8.2   Drifts og nødstopps prosedyre

Se kapittel 14 "Veiledning til rapport mal.
Nødstopp koordineres med labpersonell, for å unngå at man må ta en omvei via laben for nødstopp ved evakuering.
Vedlegg "Procedure for running experiments"

8.3   Opplæring av operatører

Dokument som viser Opplæringsplan for operatører utarbeides for alle forøksoppsetninger.
- *Kjøring av pumpesystem.*

Vedlegg*:* Opplæringsplan for operatører

8.4 Tekniske modifikasjoner

Vurdering: Modifikasjoner gjøres i samråd med Torbjørn Nielsen/Bård Brandåstrø

8.5 Personlig verneutstyr

- *Det er påbudt med vernebriller i sonen anlegget er plassert i.*

Vurdering: Vernebriller viktig, pga vann og hydraulikkolje under trykk.

8.6 Generelt

Vurdering: Alle forsøk kjøres med operatør til stede.

8.7 Sikkerhetsutrustning

- *Vernebriller*

8.8 Spesielle tiltak

9 TALLFESTING AV RESTRISIKO – RISIKOMATRISE

Se kapittel 14 "Veiledning til rapportmal.
Risikomatrisen vil gi en visualisering og en samlet oversikt over aktivitetens risikoforhold slik at ledelse og brukere får et mest mulig komplett bilde av risikoforhold.

IDnr	Aktivitet-hendelse	Frekv-Sans	Kons	RV
1	*Lekkasje i Hydraulikk,*	1	A	A1
2	*Fremmedlegemer i vannet*	1	A	A1
3	*Rørbrudd*	1	A	A1
4	*Roterende Aksling*	1	B	B1

Vurdering restrisiko: *Det er liten restrisiko ved forsøkene, foruten at trykksatt vann og olje fordrer bruk av vernebriller. Fremmedlegemer i vannet gir liten risiko for personskade, men kan føre til store skader på maskineri.*

10 KONKLUSJON

Riggen er bygget til god laboratorium praksis (GLP).

Hvilke tekniske endringer eller endringer av driftsparametere
vil kreve ny risikovurdering: Ingen

Apparaturkortet får en gyldighet på **4 måneder**
Forsøk pågår kort får en gyldighet på **4 måneder**

11 LOVER FORSKRIFTER OG PÅLEGG SOM GJELDER

Se http://www.arbeidstilsynet.no/regelverk/index.html
- Lov om tilsyn med elektriske anlegg og elektrisk utstyr (1929)
- Arbeidsmiljøloven
- Forskrift om systematisk helse-, miljø- og sikkerhetsarbeid (HMS Internkontrollforskrift)
- Forskrift om sikkerhet ved arbeid og drift av elektriske anlegg (FSE 2006)
- Forskrift om elektriske forsyningsanlegg (FEF 2006)
- Forskrift om utstyr og sikkerhetssystem til bruk i eksplosjonsfarlig område NEK 420
- Forskrift om håndtering av brannfarlig, reaksjonsfarlig og trykksatt stoff samt utstyr og anlegg som benyttes ved håndteringen
- Forskrift om Håndtering av eksplosjonsfarlig stoff
- Forskrift om bruk av arbeidsutstyr.
- Forskrift om Arbeidsplasser og arbeidslokaler
- Forskrift om Bruk av personlig verneutstyr på arbeidsplassen
- Forskrift om Helse og sikkerhet i eksplosjonsfarlige atmosfærer
- Forskrift om Høytrykksspyling
- Forskrift om Maskiner
- Forskrift om Sikkerhetsskilting og signalgivning på arbeidsplassen
- Forskrift om Stillaser, stiger og arbeid på tak m.m.
- Forskrift om Sveising, termisk skjæring, termisk sprøyting, kullbuemeisling, lodding og sliping (varmt arbeid)
- Forskrift om Tekniske innretninger
- Forskrift om Tungt og ensformig arbeid
- Forskrift om Vern mot eksponering for kjemikalier på arbeidsplassen (Kjemikalieforskriften)
- Forskrift om Vern mot kunstig optisk stråling på arbeidsplassen
- Forskrift om Vern mot mekaniske vibrasjoner
- Forskrift om Vern mot støy på arbeidsplassen

Veiledninger fra arbeidstilsynet
se: http://www.arbeidstilsynet.no/regelverk/veiledninger.html

12 VEDLEGG

13   DOKUMENTASJON

- Tegninger, foto, beskrivelser av forsøksoppsetningen
- Hazop_mal
- Sertifikat for trykkpåkjent utstyr
- Håndtering avfall i NTNU
- Sikker bruk av LASERE, retningslinje
- HAZOP_MAL_Prosedyre
- Forsøksprosedyre
- Opplæringsplan for operatører
- Skjema for sikker jobb analyse, (SJA)
- Apparaturkortet
- Forsøk pågår kort

14 VEILEDNING TIL RAPPORTMAL

Kap 5 Evakuering fra forsøksoppsetningen
Beskriv i hvilken tilstand riggen skal forlates ved en evakueringssituasjon.

Kap 7 Vurdering av teknisk sikkerhet
Sikre at design av apparatur er optimalisert i forhold til teknisk sikkerhet.
Identifisere risikoforhold knyttet til valgt design, og eventuelt å initiere re-design for å sikre at størst mulig andel av risiko elimineres gjennom teknisk sikkerhet.
Punktene skal beskrive hva forsøksoppsetningen faktisk er i stand til å tåle og aksept for utslipp.

7.1 Fareidentifikasjon, HAZOP
Forsøksoppsetningen deles inn i noder: (eks M*otorenhet, pumpeenhet, turbinenhet.)*
Ved hjelp av ledeord identifiseres årsak, konsekvens og sikkerhetstiltak. Konkluderes det med at tiltak er nødvendig anbefales disse på bakgrunn av dette. Tiltakene lukkes når de er utført og Hazop sluttføres.
(eks "No flow", årsak: rør er deformert, konsekvens: pumpe går varm, sikkerhetsforanstaltning: måling av flow med kobling opp mot nødstopp eller hvis konsekvensen ikke er kritisk benyttes manuell overvåkning og punktet legges inn i den operasjonelle prosedyren.)

7.2 Brannfarlig, reaksjonsfarlig og trykksatt stoff.
I henhold til Forskrift om håndtering av brannfarlig, reaksjonsfarlig og trykksatt stoff samt utstyr og anlegg som benyttes ved håndteringen

---

Brannfarlig stoff: Fast, flytende eller gassformig stoff, stoffblanding, samt stoff som forekommeri kombinasjoner av slike tilstander, som i kraft av sitt flammepunkt, kontakt med andre stoffer, trykk, temperatur eller andre kjemiske egenskaper representerer en fare for brann.

Reaksjonsfarlig stoff: Fast, flytende, eller gassformig stoff, stoffblanding, samt stoff som forekommer i kombinasjoner av slike tilstander, som ved kontakt med vann, ved sitt trykk, temperatur eller andre kjemiske forhold, representerer en fare for farlig reaksjon, eksplosjon eller utslipp av farlig gass, damp, støv eller tåke.

Trykksatt stoff: Annet fast, flytende eller gassformig stoff eller stoffblanding enn brann- eller reaksjonsfarlig stoff, som er under trykk, og som derved kan representere en fare ved ukontrollert utslipp.

Nærmere kriterier for klassifisering av brannfarlig, reaksjonsfarlig og trykksatt stoff er fastsatt i vedlegg 1 i veiledningen til forskriften "Brannfarlig, reaksjonsfarlig og trykksatt stoff"
http://www.dsb.no/Global/Publikasjoner/2009/Veiledning/Generell%20veiledning.pdf
http://www.dsb.no/Global/Publikasjoner/2010/Tema/Temaveiledning_bruk_av_farlig_stoff_Del_1.pdf

Rigg og areal skal gjennomgås med hensyn på vurdering av Ex sone

- Sone 0: Alltid eksplosiv atmosfære, for eksempel inne i tanker med gass, brennbar væske.
- Sone 1: Primær sone, tidvis eksplosiv atmosfære for eksempel et fylle tappe punkt
- Sone 2: Sekundert utslippssted, kan få eksplosiv atmosfære ved uhell, for eksempel ved flenser, ventiler og koblingspunkt

7.4 Påvirkning av ytre miljø

Med forurensning forstås: tilførsel av fast stoff, væske eller gass til luft, vann eller i grunnen støy og rystelser påvirkning av temperaturen som er eller kan være til skade eller ulempe for miljøet.
Regelverk: http://www.lovdata.no/all/hl-19810313-006.html#6
NTNU retningslinjer for avfall se: http://www.ntnu.no/hms/retningslinjer/HMSR18B.pdf

7.5 Stråling

Stråling defineres som

Ioniserende stråling: Elektromagnetisk stråling (i strålevernsammenheng med bølgelengde <100 nm) eller hurtige atomære partikler (f.eks alfa- og beta-partikler) som har evne til å ionisere atomer eller molekyler
Ikke-ioniserende stråling: Elektromagnetisk stråling (bølgelengde >100 nm), og ultralyd1, som har liten eller ingen evne til å ionisere.
Strålekilder: Alle ioniserende og sterke ikke-ioniserende strålekilder.
Ioniserende strålekilder: Kilder som avgir ioniserende stråling, f.eks alle typer radioaktive kilder, røntgenapparater, elektronmikroskop
Sterke ikke-ioniserende strålekilder: Kilder som avgir sterk ikke-ioniserende stråling som kan skade helse og/eller ytre miljø, f.eks laser klasse 3B og 4, MR2-systemer, UVC3-kilder, kraftige IR-kilder4
[1] Ultralyd er akustisk stråling ("lyd") over det hørbare frekvensområdet (>20 kHz). I strålevernforskriften er ultralyd omtalt sammen med elektromagnetisk ikke-ioniserende stråling.
[2] MR (eg. NMR) - kjernemagnetisk resonans, metode som nyttes til å «avbilde» indre strukturer i ulike materialer.
[3] UVC er elektromagnetisk stråling i bølgelengdeområdet 100-280 nm.
[4] IR er elektromagnetisk stråling i bølgelengdeområdet 700 nm – 1 mm.

For hver laser skal det finnes en informasjonsperm(HMSRV3404B) som skal inneholde:
- Generell informasjon
- Navn på instrumentansvarlig og stedfortreder, og lokal strålevernskoordinator
- Sentrale data om apparaturen
- Instrumentspesifikk dokumentasjon
- Referanser til (evt kopier av) datablader, strålevernbestemmelser, o.l.
- Vurderinger av risikomomenter
- Instruks for brukere
- Instruks for praktisk bruk; oppstart, drift, avstenging, sikkerhetsforholdsregler, loggføring, avlåsing, evt. bruk av strålingsmåler, osv.
- Nødprosedyrer

Se ellers retningslinjen til NTNU for laser: http://www.ntnu.no/hms/retningslinjer/HMSR34B.pdf

7.6 Bruk og behandling av kjemikalier.
Her forstås kjemikalier som grunnstoff som kan utgjøre en fare for arbeidstakers sikkerhet og helse.
Se ellers: http://www.lovdata.no/cgi-wift/ldles?doc=/sf/sf/sf-20010430-0443.html
Sikkerhetsdatablar skal være i forøkenes HMS perm og kjemikaliene registrert i Stoffkartoteket.

Kap 8 Vurdering av operasjonell sikkerhet
Sikrer at etablerte prosedyrer dekker alle identifiserte risikoforhold som må håndteres gjennom operasjonelle barrierer og at operatører og teknisk utførende har tilstrekkelig kompetanse.

8.1 Prosedyre Hazop
Prosedyre-HAZOP gjennomføres som en systematisk gjennomgang av den aktuelle prosedyren ved hjelp av fastlagt HAZOP-metodikk og definerte ledeord. Prosedyren brytes ned i enkeltstående arbeidsoperasjoner (noder) og analyseres ved hjelp av ledeordene for å avdekke mulige avvik, uklarheter eller kilder til mangelfull gjennomføring og feil.

8.2 Drifts og nødstopp prosedyrer
Utarbeides for alle forsøksoppsetninger.
Driftsprosedyren skal stegvis beskrive gjennomføringen av et forsøk, inndelt i oppstart, under drift og avslutning. Prosedyren skal beskrive forutsetninger og tilstand for start, driftsparametere med hvor store avvik som tillates før forsøket avbrytes og hvilken tilstand riggen skal forlates.
Nødstopp-prosedyre beskriver hvordan en nødstopp skal skje, (utført av uinnvidde),
hva som skjer, (strøm/gass tilførsel) og
hvilke hendelser som skal aktivere nødstopp, (brannalarm, lekkasje).

Kap 9 Risikomatrise

9 Tallfesting av restrisiko, Risikomatrisen

For å synliggjøre samlet risiko, jevnfør skjema for risikovurdering, plottes hver enkelt aktivitets verdi for sannsynlighet og konsekvens inn i risikomatrisen. Bruk aktivitetens IDnr.
Eksempel: Hvis aktivitet med IDnr. 1 har fått en risikoverdi D3 (sannsynlighet 3 x konsekvens D) settes aktivitetens IDnr i risikomatrisens felt for 3D. Slik settes alle aktivitetenes risikoverdier (IDnr) inn i risikomatrisen.

I risikomatrisen er ulike grader av risiko merket med rød, gul eller grønn. Når en aktivitets risiko havner på rød (= uakseptabel risiko), skal risikoreduserende tiltak gjennomføres. Ny vurdering gjennomføres etter at tiltak er iverksatt for å se om risikoverdien er kommet ned på akseptabelt nivå.

KONSEKVENS	**Svært alvorlig**	E1	E2	E3	E4	E5
	Alvorlig	D1	D2	D3	D4	D5
	Moderat	C1	C2	C3	C4	C5
	Liten	B1	B2	B3	B4	B5
	Svært liten	A1	A2	A3	A4	A5
		Svært liten	Liten	Middels	Stor	Svært Stor
		SANSYNLIGHET				

Prinsipp over akseptkriterium. Forklaring av fargene som er brukt i risikomatrisen.

Farge		Beskrivelse
Rød		Uakseptabel risiko. Tiltak skal gjennomføres for å redusere risikoen.
Gul		Vurderingsområde. Tiltak skal vurderes.
Grønn		Akseptabel risiko. Tiltak kan vurderes ut fra andre hensyn.